Mixed-Metal MOFs: Unique Opportunities in Metal-organic Framework Functionality and Design

Mohammad Yaser Masoomi,[a] Ali Morsali*,[a] Amarajothi Dhakshinamoorthy,[b] Hermenegildo Garcia*[c]

[a]Department of Chemistry, Faculty of Sciences, Tarbiat Modares University, P.O. Box 14155-4838, Tehran, Iran. Email: morsali_a@modares.ac.ir

[b]School of Chemistry, Madurai Kamaraj University, Madurai-625 021, India. E-mail: admguru@gmail.com

[c]Dep. de Quimica y Instituto Universitario de Tecnologia Quimica (CSIC-UPV), Valencia, 46022, Spain. E-mail: hgarcia@qim.upv.es

Abstract

Mixed-metal metal organic frameworks (MM-MOFs) can be considered those MOFs having two metals anywhere in the structure. The present review summarizes the various strategies reported for preparation of MM-MOFs and some of their applications in adsorption, gas separation and catalysis. It is shown that compared to homometallic MOFs, MM-MOFs bring about the opportunity to take advantage of the complexity and the synergism derived from the presence of different metal ions in the structure of MOFs. This is reflected in a superior performance and even stability of MM-MOFs respect to related single metal MOFs. Emphasis is made on the use of MM-MOFs as catalysts for tandem reaction.

Keywords: Mixed-metal; Heterogeneity; Metal Organic Frameworks; Solid solution; Metal nanoparticle

1 Introduction

In the past decade, considerable attention has been paid to metal-organic frameworks (MOFs) which are constructed by connecting metal-containing nodes (secondary building units (SBUs)) with rigid multipodal organic linkers through strong bonds (reticular synthesis).[1-5] The ability to design and use different SBUs and ditopic or polytopic organic linkers results in the construction of a large diversity MOFs whose composition and properties can be adapted to specific applications.[6-11]

Due to simplicity the vast majority of the MOFs reported so far have homometallic SBUs.[12, 13] The condition of reversibility in the metal-ligand coordination required to obtain highly crystalline materials can be easier achieved for only one type of metal ion. In addition, the clusters of single metal ions appearing during the early stages of the synthesis may exhibit certain preferred coordination geometries resulting in periodic reticulation forming a crystalline solid rather than an amorphous phase.[14]

Starting from the current knowledge on the synthesis mechanism and procedures for post-synthetic modification, a logical evolution in the area is to increase further the complexity of MOF structures to obtain a new generation of materials with improved performance. The term "*heterogeneity*" in MOFs will be used hereafter to denote the presence of several types of SBUs and/or covalently linked functionalities within the crystal periodic structure of the MOF. The term *heterogeneity* will also include possible structural defects such as vacancies, multiple metal ions, and hierarchical pore sizes (micro, meso and macro), the challenge being to maintain lattice order and preserve crystallinity in the MOFs, while introducing heterogeneity in a controlled way, providing convincing evidence on material characterization at atomic level.[15]

Chen and coworkers have defined *mixed-metal* MOFs (MM-MOFs) as those MOFs having two metals anywhere in the structure.[16] The presence of more than one metal in the nodes or immobilization of metal ions, metal nanoparticles, metal complexes, and organometallic compounds inside MOF cavities as guests with or without interaction with the MOF framework are particular cases of heterogeneity in MOFs and according to Chen's definition of MM-MOFs will be the subject of the present review. [17-22] These MOFs containing more than one metal somewhere in their structure offer opportunities in terms of multifunctionality and tuning of the properties of the material to a given application. Due to the synergistic effects that could derive from the presence of two or more metals, MM-MOFs can exhibit better performance in various applications compared to single-metal MOFs particularly in gas storage and separation, heterogeneous catalysis, sensing, and construction of photoactive materials. [23, 24] Particularly in the field of heterogeneous catalysis, MM-MOFs offer the possibility to have two centers of different catalytic activity in close spatial proximity. These multifunctional catalysts are specially suite to promote tandem or cascade reactions, where two or more individual reactions are combined in a single process. Tandem reactions are examples of process intensification, minimizing in a process the number of steps, mixture separation and workup. MM-MOFs may also have improved thermal and water stability, [25] increasing the robustness of the structure making it suitable for more extensive applications. It is also important to gain understanding on the factors governing the preparation of these MM-MOFs. Since the number of reported MM-MOFs and their applications have been growing very recently, it is particularly timely to provide a minireview on this area complementing those already existing in the literature.[16, 26, 27]

2 Synthetic strategies for preparation of MM-MOFs

MOFs are synthesized following a large variety of procedures, including solvo/hydro thermal method, slow diffusion, conventional heating, slow evaporation, mechanochemical, sonochemical, etc.[28-32] Several of these synthetic strategies have been also applied to the fabrication of MM-MOFs. In principle, all these strategies can be classified either into one-pot synthesis or post-synthesis modification.

2.1 One-pot synthesis of MM-MOFs using mixtures of different metal precursors

Appropriate mixtures of different metal precursors have been reported for the direct synthesis of MM-MOFs (Figure 1). [33-37] The main attractiveness of this approach is the simplicity and the reduced number of steps, however the main disadvantage of this strategy is in general the lack of control over the final metal distribution. However, the possibility that only one of the metals is really incorporated at the nodes, while the second one is present in satellite nodal positions or in a different phase as small (hydroxy)oxide clusters has to be seriously considered. Advanced characterization techniques such as XANES and EXAFS are necessary to convincingly prove the success of the one.pot MM-MOF synthesis.

As a rule of thumb, the success of this methodology relies in the use of metal ions with the same Coulombic charge, ionic radius, and similar chemical behavior to enhance the production of homogeneous co-incorporation of the different metals in the framework structure. However, by employing hetero multitopic linkers it could be possible to prepare MM-MOFs with metal ions of different softness/hardness that would not be formed using the most common multitopic linkers. In this way, ligands having different donor atoms can coordinate metal ions of different Lewis

acidity and coordination geometry forming a MM-MOF. [23, 38-41] MM-MOFs in which two metals are presented in certain proportion range have been reported to be prepared using synthetic procedures common in MOF synthesis, such as conventional heating and solvothermal procedures. [17, 42-49] Depending on the synthesis conditions and the nature and proportion of the various metal precursors the resulting MM-MOF can derived from the thermodynamic or kinetic control and this may influence the distribution and location of the metals. Considering the possible differences, the synthetic procedures should screen a variety of conditions, determining the influence of various parameters in the final MM-MOF.

MM-MOFs with the same metal in mixed-valence states have also been reported directly in one-step synthesis. [50-56] Anionic frameworks can be considered another type of MM-MOFs in which metal ions are present in the pores as charge-balancing cations to compensate for the lattice charge.[20]

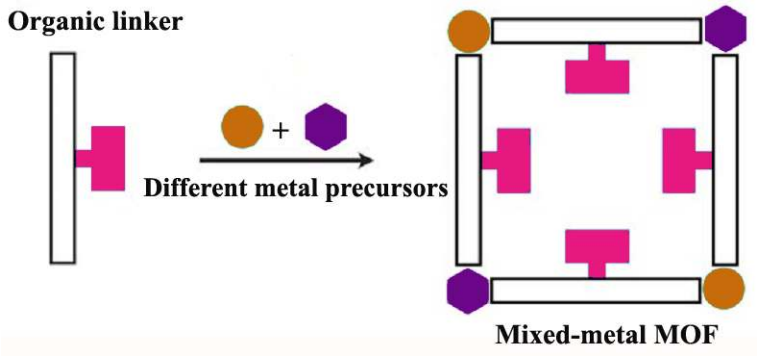

Figure 1. Sketch illustrating the direct synthesis of MM-MOFs using two metals.

Regarding structural stability, Stock and co-workers have prepared a series of bimetallic Ce/Zr-UiO-66 and Ce/Zr-MOF-808 solids of various Ce^{4+} to Zr^{4+} ratios.[57] The experimental results have convincingly proved that those solid samples with Ce ≤ 20 at% exhibited an enhanced thermal stability as well as higher resistance against acids. Although the preparation of these types

of MM-MOFs has been optimized and their thermal and chemical stability have been demonstrated, the applications of these MM-MOFs in organic transformations are still lacking. It is interesting to note that Ce^{4+} salts have been extensively employed as a homogeneous catalysts for a wide range of reactions in organic synthesis.[58]

2.2 Using metalloligands

Another approach for the direct synthesis of MM-MOFs is the use of linkers that already contain a second metal complexed (*metalloligands*) compatible with the MOF synthesis conditions. This approach is certainly one of the most convenient methodologies to immobilize metallic complexes and prepare porous MM-MOFs, although it has the limitation of the presence of two different metal sites, either at the lattice nodes or at the linker in satellite positions. As shown in Figure 2, the key point is the use of a metalloligand to specifically coordinate with one metal ion type to form MM-MOFs. This approach can rationally immobilize different metal sites straightforwardly into the MM-MOFs. [22, 59-61]

This strategy is based on preformed metallocomplexes as linkers bringing access to a broad new class of MM-MOFs. This approach renders MM-MOFs with accessible metal complexes immobilized in large and extra-large channels that can exhibit high stability against complex agglomeration that is a common deactivation process occurring for these soluble metal complexes.

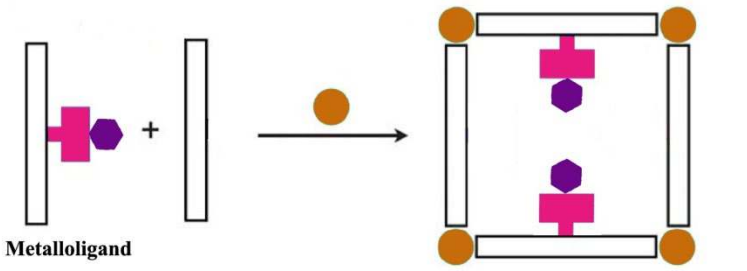

Figure 2. Schematic representation of the synthesis of MM-MOFs using metalloligands.

An alternative to the direct MM-MOF synthesis involving the preformed metallocomplex as linker is a two-step procedure consisting of the preparation of a single metal MOF with the corresponding bifunctional ligand that subsequently forms the complex with a second metal ion resulting in the MM-MOF (Figure 3). [38, 62-67] This two-step procedure can be more general and can serve for those cases in which the preformed complex would not survive to the conditions required in a one-pot reaction. Also, two step mechanochemical syntheses have been reported for the synthesis of MM-MOFs with controllable stoichiometric composition.[68] Considering the simplicity of mechanochemical synthesis, it would be worth exploring the general applicability of this strategy to the preparation of MM-MOFs.

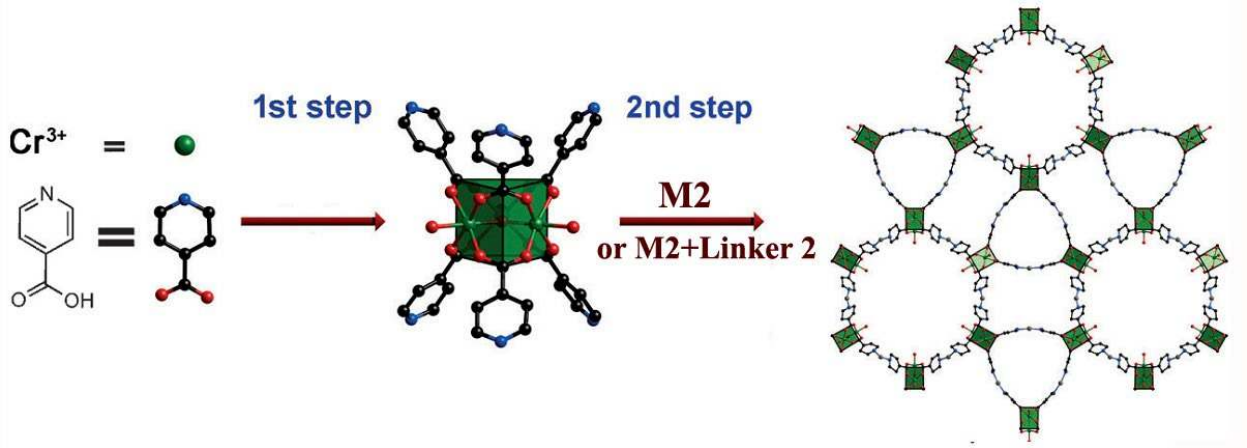

Figure 3. Schematic illustration of the two-step synthesis of MM-MOFs by first forming the solid with a linker able to bind a second type of metal. Ref [[62]]

A relevant example of the MM-MOF synthesis based on metalloligands is the use of porphyrin linkers to obtain multivariate MM-MOFs (MTV-MOFs). Porphyrin linkers can be

conveniently employed as linkers in the construction of these MTV-MOFs.[69-71] Multivariate MOFs can be defined as MM-MOFs where the composition of the metal nodes changes in a defined way within the solid. Thus, a series of MTV-MOFs have been reported by combining various metal ions at the metal oxide nodes acting as SBUs (Figure 4a). In some of the examples of multivariate MM-MOFs, the structure is composed of two SBUs. The first one is the domain arrangement in which each of two different SBUs are constructed by three ions of the same metal and expanded in a certain area of the structure. The other order is a well-mixed arrangement wherein two different metals are in the same SBU which are spread out throughout the whole MM-MOF structure (Figure 4b). These two types of SBU arrangements also influence the properties and reactivity of MM-MOFs so that in certain domains the band structure is very similar to the single component MOF, while the band gaps are changed greatly in the well-mixed arrangement. [71]

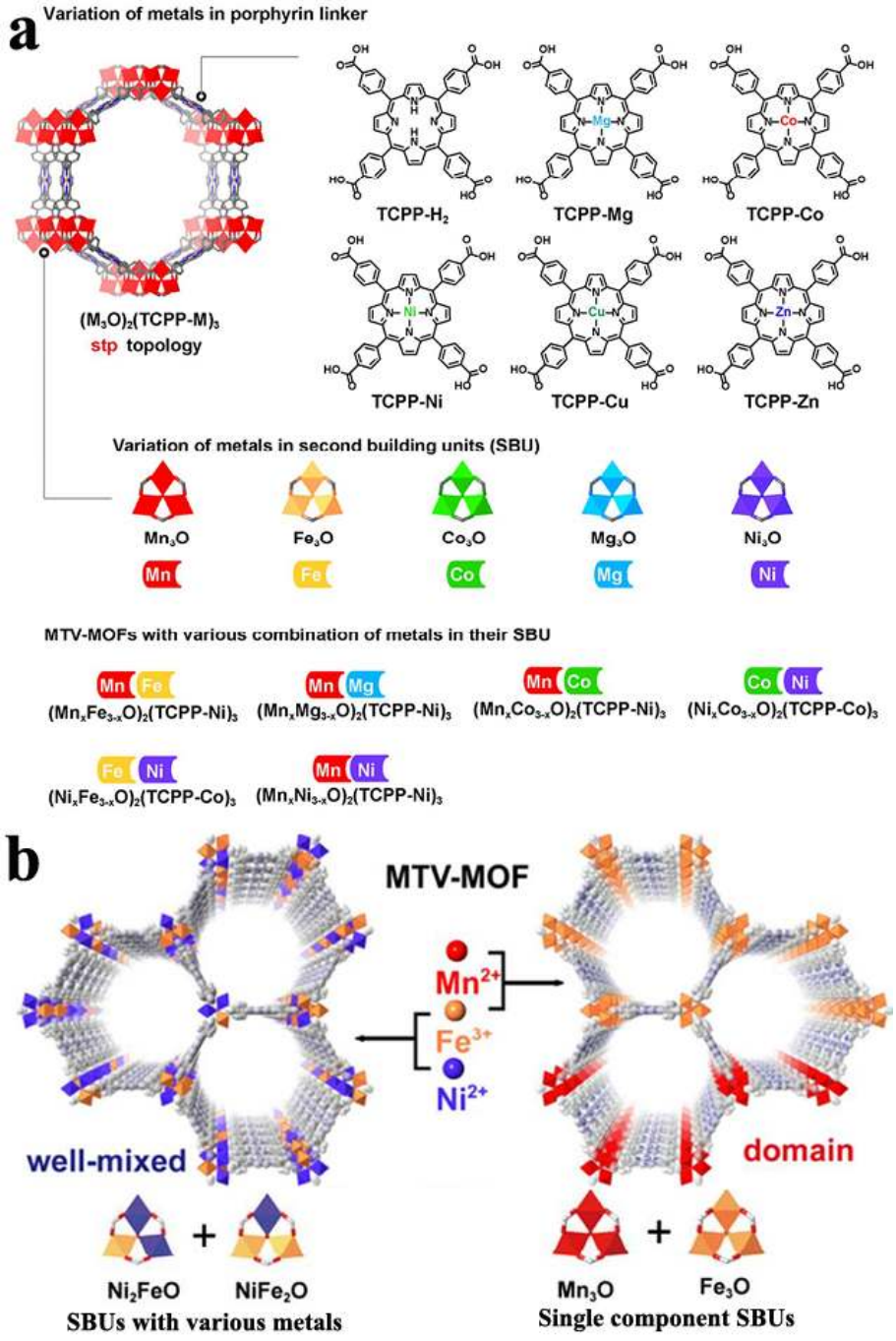

Figure 4. (a) Single component MOF series, $(M_3O)_2(TCPP\text{-}M)_3$, constructed by five different SBUs and six different porphyrin linkers, and MTV-MOFs with mixed-metal SBUs. (b) Two arrangements in MM-MOFs and their SBUs. (TCPP = tetrakis (4-carboxyphenyl) porphyrin) [[71]]

2.3 Post-Synthetic Modification (Transmetalations)

Post-synthetic approaches are useful strategies as they can provide the targeted heterometallic MM-MOFs which cannot be achieved through *de novo* synthesis due to the different reactivity of the metal ions. Post-synthetic modification can include the exchange of metal nodes in the structure, new metal insertion, or even epitaxial growth modification. By post-synthetic modification, different percentages of new metals may be included in the new MM-MOF.[33, 72] Control over the amount of second or third metals that are incorporated into the framework of MM-MOF can tune the MOF properties for specific applications. However, as commented in the previous section, evidence of post-synthetic modifications should not be based exclusively on chemical analysis of the solid and solutions, advanced structural characterization techniques being necessary to support the success of the modification on firm ground.

2.3.1 Epitaxial growth on the MOF surface

In some cases a MOF with a new metal ion can grow epitaxially on the surface of another MOF by using crystals of a core MOF as seeds in a solution of different metal ion resulting in a core–shell MM-MOF. Typically in the core−shell MM-MOF, MOF_{shell} with the M2 metal center is formed on the surface of MOF_{core} with M1 metal center ($MOF_{core, M1}$@$MOF_{shell, M2}$) with the same organic linker (Figures 5 and 6). [73, 74]. These core–shell MOFs have some resemblance to solid solutions in which the lattice parameters of two parent crystal structures have a good match. There are only a few examples of core−shell MM-MOFs, [73, 74] although due to the remarkable structuration of the particles that can be achieved by this methodology, it would be interesting to explore further the property of this type of core-shell MM-MOFs.

In this $MOF_{core}@MOF_{shell}$, generally the lattice parameters of the shell MOF and the core MOF need to be closely related. It should be noted that usually it is not possible to obtain MOF_{shell} as single crystal. By epitaxial growth a clear interface between the core and the shell is generally possible to be observed in the heterostructure. This methodology is an appropriate way to synthesize highly porous MTV-MOFs with framework stability and multifunctionality. It will be of interest to establish general rules allowing to predict the possibility of epitaxial growth based on the analysis of the structures and their X-ray diffraction.

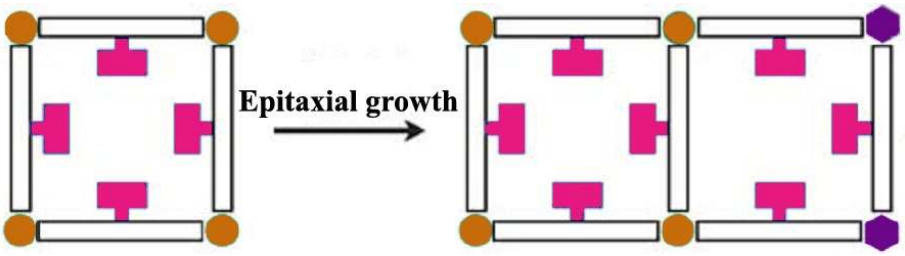

Figure 5. Schematic representation of the core–shell approach to forming MM-MOFs.

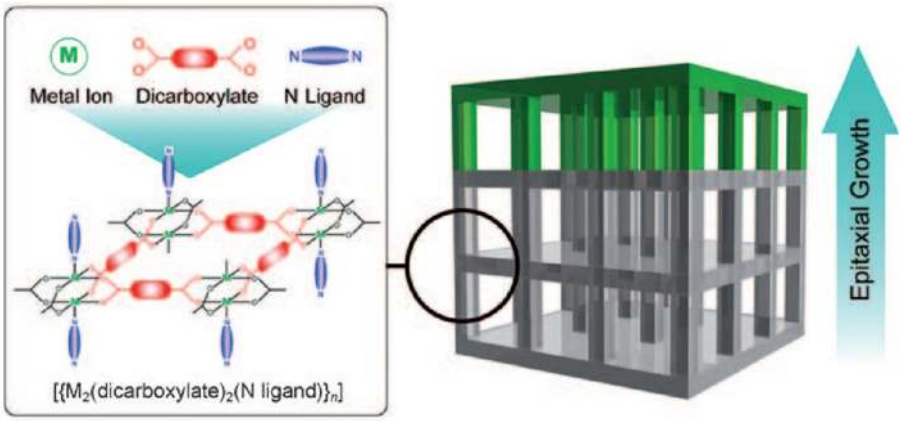

Figure 6. Schematic illustration of epitaxial growth on the MOF surface. Ref [[73]]

2.3.2 Metal elimination-addition (or Demetalation/Remetalation)

Creating ordered metal and linker vacancies in MOFs that are subsequently healed with other metal is another useful strategy for preparation of MM-MOFs (Figure 7). [75] Vacancies can be generated in the as-synthesized MOFs by elimination reactions, while they can be subsequently refilled with different metal ion in a vacancy to metal ratio that depends on the coordination mode and charge of new metal ion (Figure 8). The elimination process can also be applied to metalloligand MOFs, where other metals different to those used in the synthesis can be introduced in the healing step to produce isostructural MM-MOF materials (Figure 9). [76]

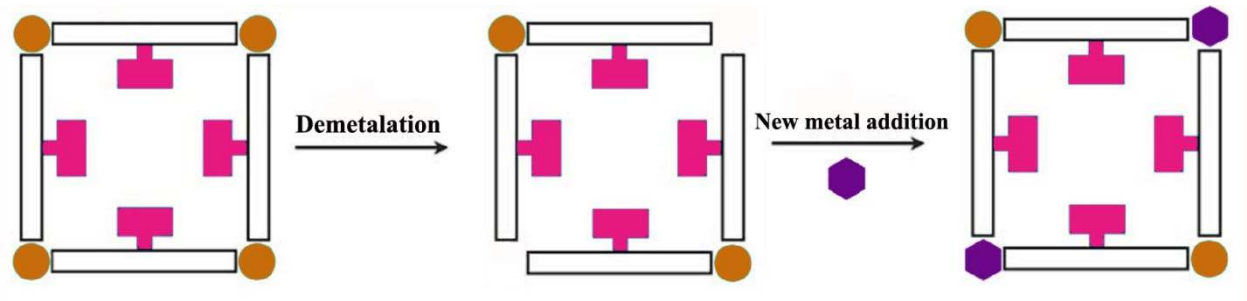

Figure 7. Schematic representation of the formation of a MM-MOF through post-synthetic demetalation and subsequent remetalation.

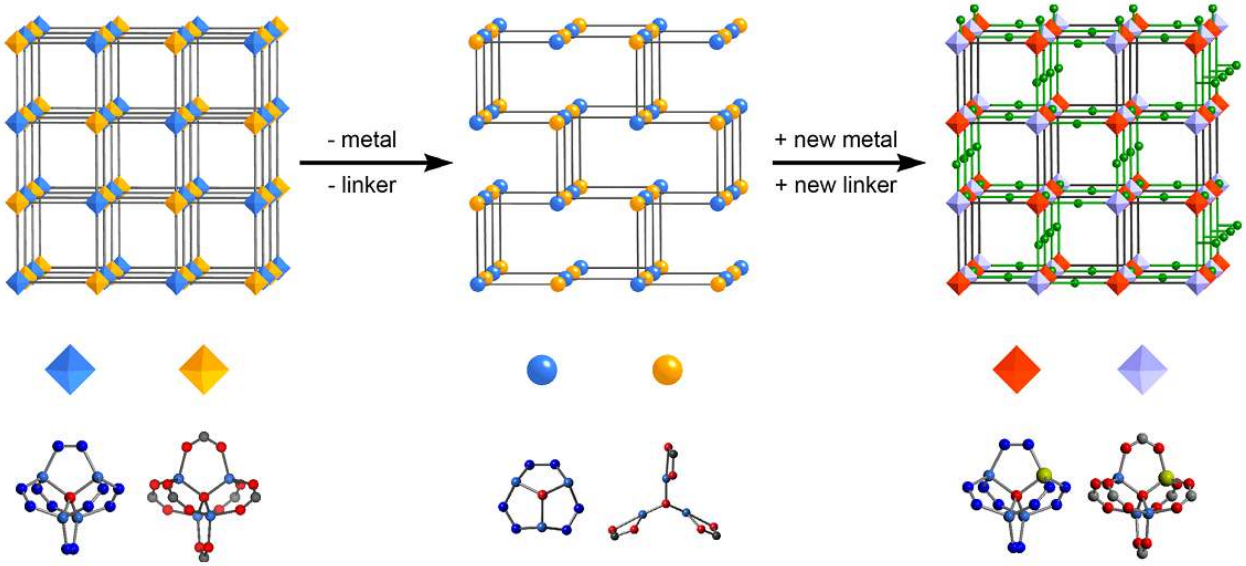

Figure 8. Illustration of the generation of metal and linker vacancies in MOF followed by reconstruction of the structure with new metal and new linker. Ref [[75]]

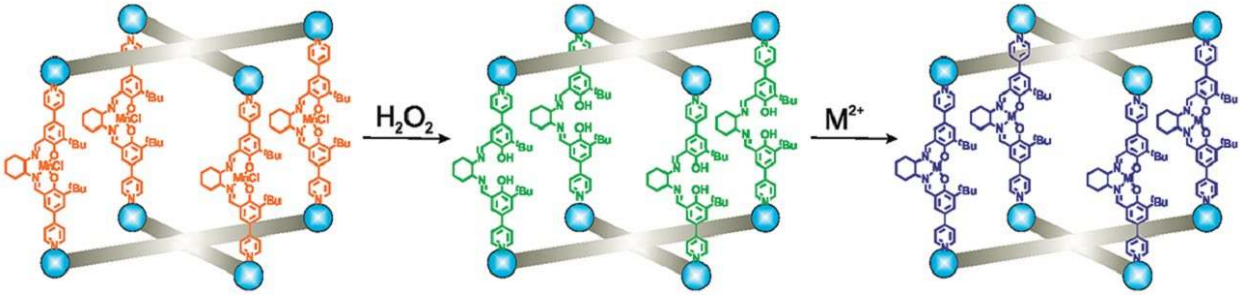

Figure 9. Schematic illustration for demetalation of a metallosalen-containing MOF and its subsequent remetalation with a different metal.[[76]]

2.3.3 Metal exchange

Metal exchange is often carried out by stirring the homometallic parent MOF with the second metal of choice in a liquid solution in which partial replacement of metal in parent MOF

can be tuned by controlling synthetic parameters such as concentration, reaction time and exchange temperature (Figure 10). [21, 74, 77-80] The possibility of the metal exchange to prepare MM-MOF is based on the well-established reversibility of the metal-ligand bond that is behind the synthesis of MOFs with high crystallinity and the use of modulators.[81] One of the most widely reported metal replacement corresponds to Zr-based MOFs that are modified by exchange with Ti(IV) or Hf(IV) ions (Figure 11). [82] Evidence in favor of the success of the ion exchange is mainly based on chemical analysis of the liquid as well as the MM-MOF. However, this data are insufficient to locate the exchanged sites and much more detailed structural characterization is needed. Thus, in the case of Ti(IV), recent characterization by TEM-EDX has cast doubts about the success of the nodal Zr-by-Ti exchange and it was proposed that the Ti(IV) species become attached to linker vacancies in the structure.[83] Further exhaustive characterization appears pertinent to clarify the conditions for a real post-synthetic nodal metal exchange.

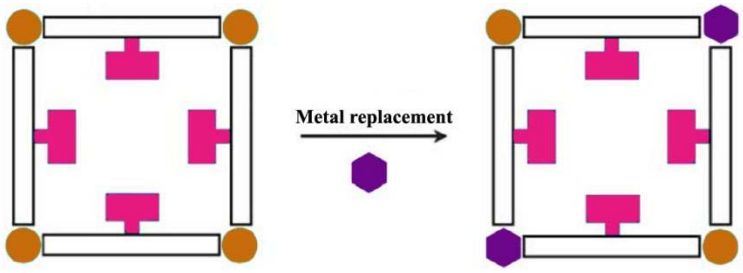

Figure 10. MM-MOF formation through post-synthetic partial metal exchange.

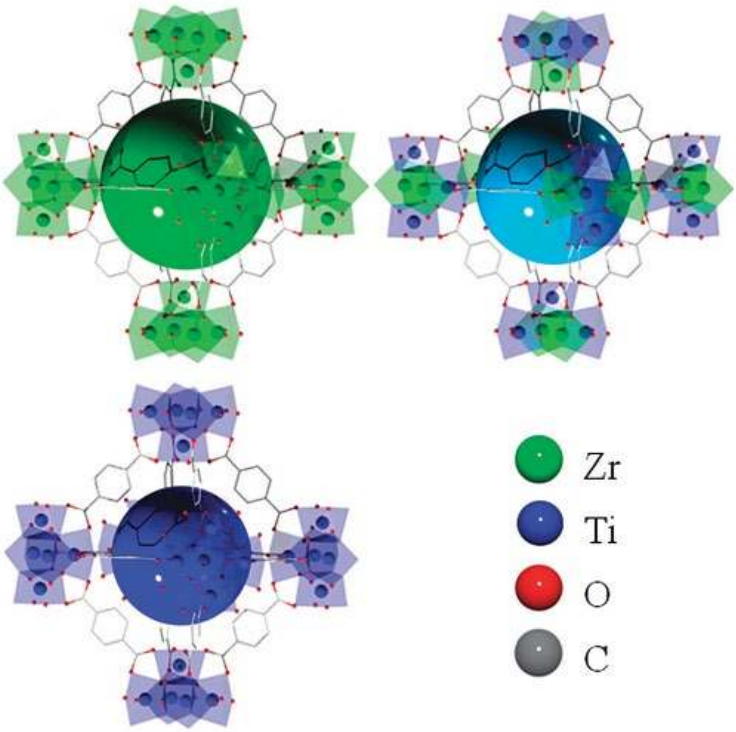

Figure 11. Post-synthetic partial metal exchange in UiO-66(Zr) with Ti(IV) to form UiO-66(Zr/Ti). Ref [[21]]

Interestingly, during the partial metal exchange in MOF crystals, a core−shell MM-MOF structure can be formed because that metal replacement proceeds from the crystal surface towards the core (Figure 12). In this way, post-synthetic ion exchange provides a route to synthesize core−shell MM-MOFs that could not be accessed via epitaxial growth. As shown in Figure 12, it is possible to grow epitaxially MM-MOFs via metal node exchange in MOFs constituted by either Ni^{2+}, Co^{2+} or Cu^{2+} metal ions by immersing the initial MOF in a solution containing Zn^{2+}. [72, 74]

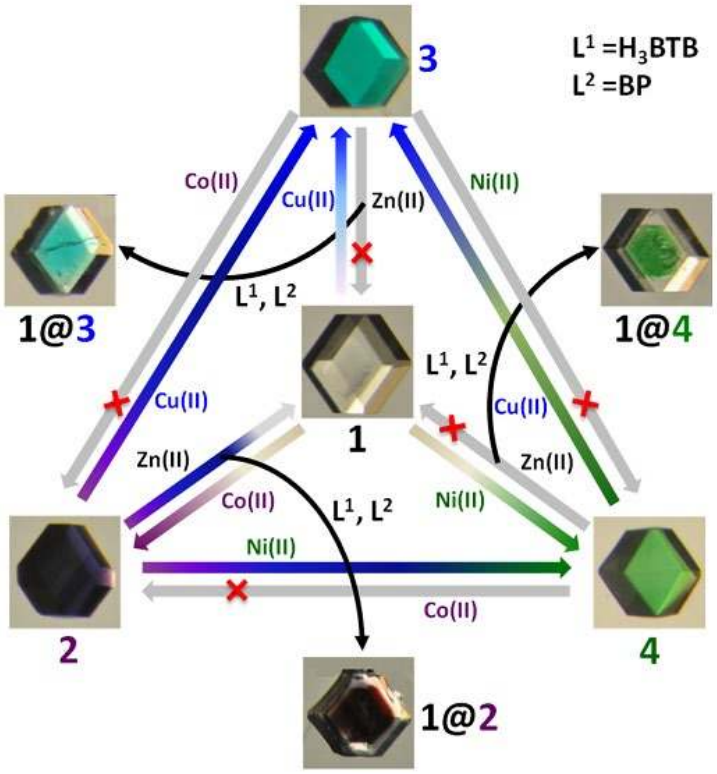

Figure 12. Formation for core−shell MM-MOF by ion exchange. Ref[[74]]

2.3.4 Metal Insertion

Metal insertion is a convenient method to obtain various MM-MOFs that can be applied in various MOF materials (Figure 13). In homometallic anionic-framework MOFs the desired different metal ions can be inserted by cation exchange.[84-86] Also, appropriate functional groups (e.g. chelating sites, thioether functional group, etc.) in MOFs can load metal ions or lead to the inclusion of metal complexes by soaking the parent MOF in solutions of metal ions or complexes (Figure 14).[86-89]

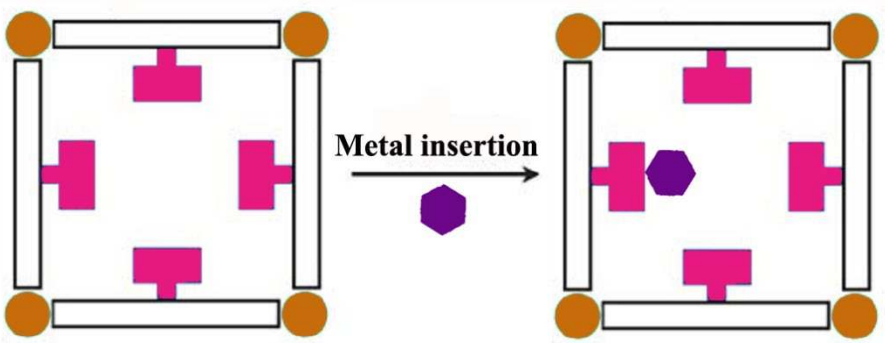

Figure 13. Formation of MM-MOF through post-synthetic metal complexation.

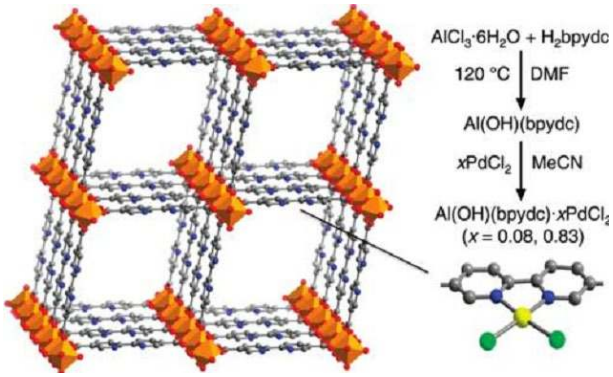

Figure 14. Insertion of $PdCl_2$ into open BPYDC (BPYDC = 2,2'-bipyridyl-5,5'-dicarboxylic acid) ligand sites. Ref [[87]]

Loading of metal nanoparticles or organometallic compounds in MOF cavities is another type of metal insertion which according to the adopted definition of these materials also leads to the preparation of MM-MOFs. [90-93] After inclusion of metal ions into the MOF pores, metal nanoparticles inside of MOF cavities will be obtained by applying reducing reagent or photoreduction.[94, 95] Moreover, chemical or electrochemical reduction of MOFs using organometallic reducing agents or by applying negative potentials in an electrode leads to the preparation of mixed-valence MOFs which can subsequently uptake in the cavities new metal ions or organometallic complexes. [96, 97]

3 MM-MOFs properties and applications

MM-MOFs as examples of MTV-MOFs may offer several advantages over homometallic MOFs by providing complexity and introducing functionality derived from the different metal ions in the MOF structure. The presence of different metals affects the properties and may expand the applications of MOFs. MM-MOFs exhibiting framework stability and multifunctionality may perform better than traditional MOFs due to the complementarity and synergy of two different metals. In general, any application related to the activity of metal centers will be affected by the presence of different metals and their ratio. This section provides examples to illustrate the improved performance and new properties of MM-MOFs compared to related homometallic analogs. The examples have been grouped according to the location of the different metals and the type of MM-MOF.

3.1 MM-MOFs with metals in nodal positions and Mixed-Valence MM-MOFs

MM-MOFs show some exceptional properties that can be considered somehow analogous to those found in solid solutions, whose behavior is related to the type and ratio of transition metals.[18, 98]

Interestingly, the mixed-metal analogs of some MOF structures such as MIL-101 and MIL-88 that are built by trimetallic-μ_3-oxo clusters may exhibit higher porosity when one of the metal cations bears two instead of three positive charges as consequence of the absence of charge-compensating anions that otherwise are needed in conventional homometallic MOFs and occupy some internal volume.[19] This strategy based on mixed metal clusters can be used to achieve a better control over the porosity and surface area of MOFs by employing simple stimulant terminal

ligands (pyrazole, pyridine and bipyridine). In the absence of the stimulant ligand, the MM-MOF can be in a dense form without porosity, while the binding of the stimulant ligand to the nodes can open the structure and generate porosity. In this way, the use of stimulant ligands of different molecular size could result in the switchable and reversible three-level porosity (Figure 15). Different porous levels could be tailored depending on the choice of the stimulant terminal ligand. One of the striking features of Fe_2Ni-MIL-88B is its switchable porosity and specific surface area (30 m^2g^{-1} to 1120 m^2g^{-1}) and pore volume (10×10^{-3} cm^3g^{-1} to 448×10^{-3} cm^3g^{-1}). Hence, the resulting materials are expected to have significant applications in adsorption and separation in which the pore size of the material can be reversibly controlled depending upon the required application. There are enormous opportunities for construction of a large variety of mixed metal MOFs with improved properties by appropriate choice of trimeric tri-/dipositive mixed metal clusters $M_2^{III}M^{II}$-μ_3O (M^{III}= Fe, Cr, Mn, Rh and M^{II} = Ca, Ba, Mg, Ni, Mn, Co) and the selection of terminal ligands across N-donor, S-donor and O-donor ligands.

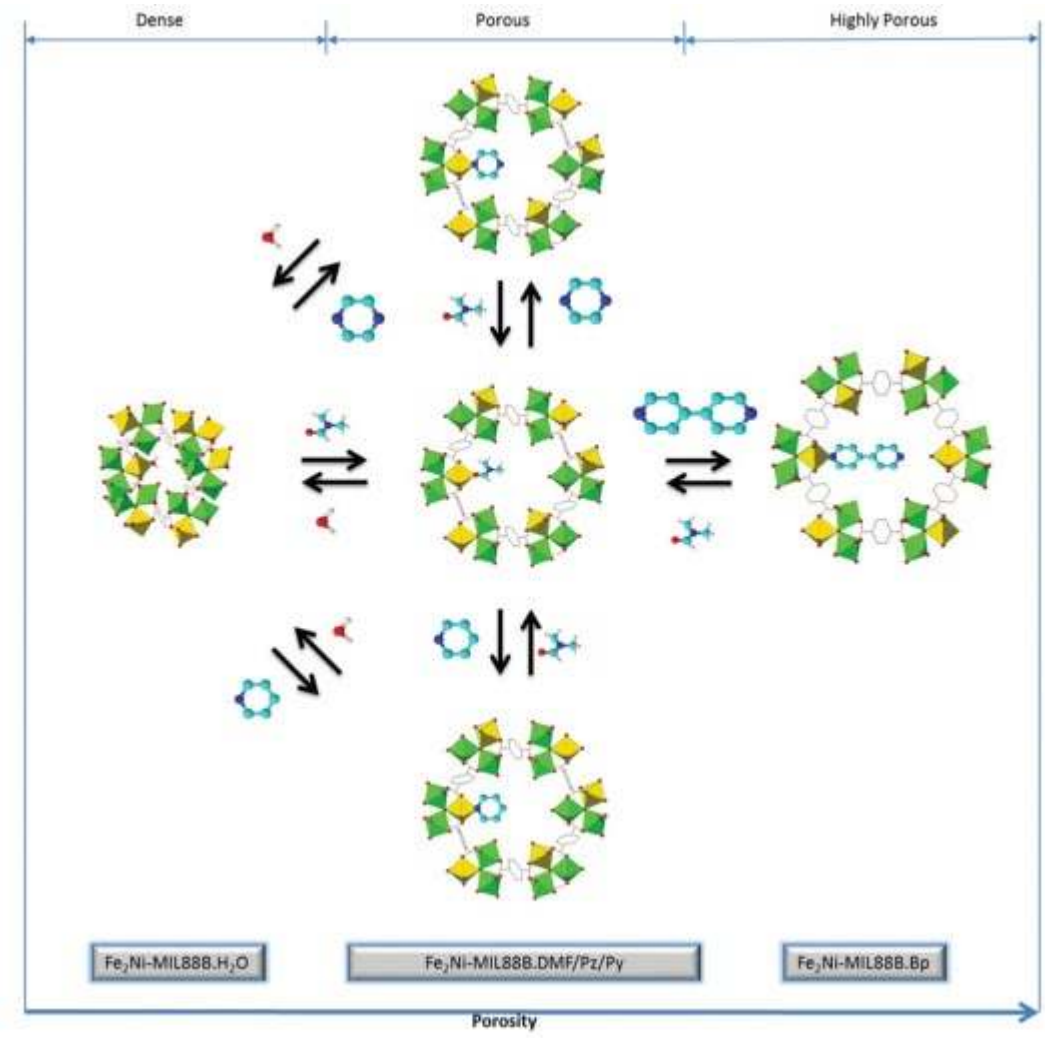

Figure 15. Reversible ligand exchange and porosity control of Fe_2Ni-MIL-88B, for clarity, only terminal ligands bonding to Ni are shown. Ref [19]

MM-MOFs can be applied as precursors for preparation of binary, ternary and quaternary mixed metal oxide nanoparticles which have a wide variety of important physical properties and applications. As it is difficult to control the stoichiometry and size of the mixed-metal oxides, one general strategy to prepare these nanoparticles is based on the use of MM-MOF that are subsequently decomposed. [99, 100] For instance a pure $ZnCo_2O_4$ phase with a high surface area (55

cm^2 g^{-1}) has been obtained from a Zn^{2+} and Co^{2+} MM-MOF $ZnCo_2O(BTC)_2(DMF)H_2O$ (BTC: 1,3,5-benzenetricarboxylate) and applied as electrode material for supercapacitors showing high specific capacitance of 451 F g^{-1}.[100]

MOFs are widely used as heterogeneous catalysts for wide range of reactions.[101-103] The catalytic center promoting the reaction can be the metal nodes, metal complexes encapsulated or grafted on the linkers, metal nanoparticles incorporated inside the pores or functional groups present at the organic linker. MM-MOFs which have more than one metal in their structures bring about the possibility for development of multifunctional solid catalysts with more than one type of active site at the metal node. [27] In this way, the catalytic activity of the MM-MOF can be higher than that of analogous homometallic MOFs. In one of these examples, MIL-100(Fe,Ni) exhibits enhanced activity as catalyst for the Lewis acid-catalyzed condensation of β-pinene and formaldehyde than MIL-100(Fe) due to the generation of defects in the structure.[104]

Stoichiometric MM-MOFs can catalyze various reactions such as cross condensation of benzaldehyde and cyclohexanone, cyclohexene oxidation, ring opening of styrene oxide where they have superior catalytic performance compared with homometallic MOFs. [44, 105, 106] In one of these examples, Co/NiMOF-74 was shown to be active in the oxidation of cyclohexene while no activity was observed for Ni-MOF-74. The observed activity of Co/NiMOF-74 may be explained considering that Co substitutes Ni at those positions of Ni-MOF-74 where substrates have easy accessibility. Furthermore, the mixed-metal Co/Ni-MOF-74 MOF exhibited superior activity in the oxidation of cyclohexene compared to Co-MOF-74 possessing stoichiometric Co loading.[105] These catalytic data provide another strategy to develop stoichiometric MM-MOFs for various applications including heterogeneous catalysis and emphasizing promising potentials of these materials in near future.

The influence of Fe doping in the framework of MFM-300(Ga_2) (MFM: Manchester Framework Material) was reported in the ring-opening of styrene oxide by methanol to obtain 2-methoxy-2-phenylethanol at 40 ºC.[106] A blank control experiment in the absence of any catalyst showed 4 % conversion of styrene oxide to 2-methoxy-2-phenylethanol after 30 h at 40 °C. In contrast, the ring-opening of styrene oxide with heterogeneous MFM-300(Ga_2) catalyst exhibited 40 % conversion of styrene oxide under identical conditions. Higher activity exhibited a Fe containing MFM-300(Ga_2), namely, MFM-300($Ga_{1.87}Fe_{0.13}$) that achieved quantitative styrene oxide conversion with very high selectivity to the expected product under similar conditions. Further, MFM-300($Ga_{1.87}Fe_{0.13}$) was reused for three cycles without any noticeable decay in its catalytic performance. These results were interpreted as derived from the higher Lewis acidity of Fe^{3+} combined with framework stability.

Fe@PCN-222(Fe) MM-MOFs were prepared from a bioinspired iron(III)porphyrinic Zr-MOF, PCN-222(Fe) that was treated with $FeCl_3$ via post-synthetic cluster metalation.[107] The structure of Fe@PCN-222(Fe) MM-MOFs consist of (Zr-oxo-Fe) nodes linked by Fe(III)porphyrin struts. The catalytic performance of Fe@PCN-222(Fe) was examined in the one-pot tandem synthesis of quinazolin-4(3H)-ones from benzyl alcohols and 2-aminobenzamide through a three consecutive steps involving oxidation, cyclization and oxidation under visible light irradiation using air or oxygen without adding any additive. The catalytic results indicated the superior performance of Fe@PCN-222(Fe) compared to the parent PCN-222(Fe) and the corresponding homogeneous catalysts. The catalytic data and the control experiments indicate that MM-MOFs act as both a photoredox and Lewis acid catalyst. Fe@PCN-222(Fe) was reused three cycles without loss in its activity. Hot-filtration test showed the absence of iron leaching, thus demonstrating its stability under reaction conditions. This work constitutes a clear example of the

potential of MM-MOFs to promote tandem organic transformations combining photocatalysis and catalysis with different active sites within a single framework.

A series of MM-MOFs were prepared containing Ga and In ions. These Ga-In MM-MOFs are isostructural with their homometallic MOFs. The activity of these MM-MOFs was studied in the three-component, one pot Strecker reaction.[108] InGaPF-1[$In_{0.72}Ga_{0.28}(O_2C_2H_4)_{0.5}$(hfipbb)], InGaPF-2 [$In_{0.55}Ga_{0.45}(O_2C_2H_4)_{0.5}$(hfipbb)] and InGaPF-3 [$In_{0.28}Ga_{0.72}(O_2C_2H_4)_{0.5}$(hfipbb)] ($H_2$hfipbb = 4,4'-(hexafluoroisopropylidene) bis(benzoic acid) MM-MOFs were prepared with different proportions of In and Ga occupying equivalent crystallographic sites. The Strecker reaction between benzaldehyde, aniline and trimethylsilylcyanide using InGaPF-1, InGaPF-2 and InGaPF-3 MM-MOFs afforded Strecker product in 64, 91 and 96 % yields after 96, 1.33 and 0.3 h, respectively. In contrast, homometallic GaPF-1 afforded exclusively benzaldehyde silylation, while homometallic InPF-11β favored the imine formation under identical conditions. In contrast, the physical mixture of GaPF-1 and InPF-11β MOFs gave the Strecker cyano amino product after 1 h which is a time two times longer than the time required with InGaPF-3. These results indicate that the physical mixture of individual homometallic MOFs, even though can promote the tandem reaction, is less efficient due to the distance between the active sites. Furthermore, these catalytic data clearly indicate that the addition of a small amount of indium is enough to achieve in short time the Strecker cyano product in contrast to aldehyde cyanosilylation.

In another example, MM-MOFs were prepared by replacing Sc^{3+} in MIL-100(Sc) by Fe^{3+} to obtain MIL-100(Sc,Fe), testing its activity as solid Lewis acid as well as redox reactions.[109] The structural analysis of MIL-100(Sc,Fe) catalyst are compatible with both Fe^{3+} as well as Sc^{3+} cations occupying framework sites and behave as Lewis acid catalysts (by coordination to the Sc^{3+} and Fe^{3+} ions) and oxidation catalysts (Fe^{3+} sites). In addition, the Sc,Fe MIL-100 framework was

found to be robust, highly porous with three-dimensionally connected voids. These studies have clearly demonstrated that MM-MOFs exhibit much superior activity than their corresponding homometallic MOFs with a single metal ion in the framework structure for Lewis acid catalysis, tandem C-C bond formation and alcohol oxidation.

A magnetic $CoFe_2O_4$/TMU-17-NH_2 was prepared and submitted to Cu(II) exchange to obtain $CoFe_2O_4$/[$Cu_{0.63}$/$Zn_{0.37}$-TMU-17-NH_2] MM-MOFs magnetic nanocomposite (Figure 16). The activity of the homometallic and the Cu-Zn MM-MOFs was tested in the synthesis of tetrazole derivative from benzaldehyde, hydroxylamine and sodium azide.[110] The catalytic data indicated that $CoFe_2O_4$/[$Cu_{0.63}$/$Zn_{0.37}$-TMU-17-NH_2] reaches 98% yield of tetrazole after 8 min in DMF at 120 ºC. In contrast, $CoFe_2O_4$/TMU-17-NH_2 required 30 min to give 78 % tetrazole yield under identical conditions. These catalytic data indicate that the product yield can improved by incorporation of Cu within the framework of TMU-17-NH_2. Reusability tests showed that the activity of $CoFe_2O_4$/[$Cu_{0.63}$/$Zn_{0.37}$-TMU-17-NH_2] is maintained in five cycles without any decay.

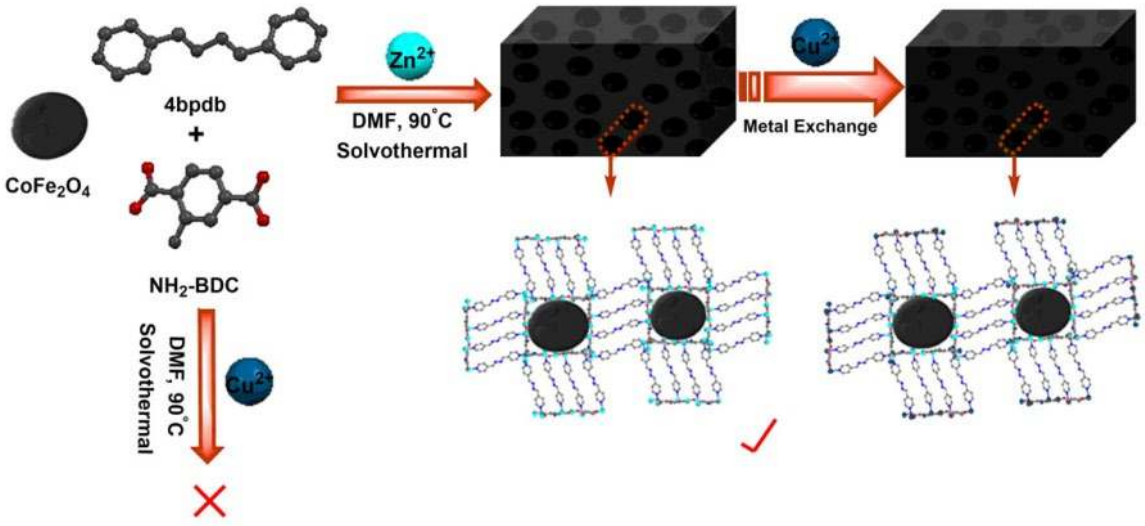

Figure 16. Preparation of $CoFe_2O_4$/[$Cu_{0.63}$/$Zn_{0.37}$-TMU-17-NH_2] MM-MOFs.

Another possible advantage of MM-MOFs in catalysis is the development of stable materials due to the presence of one metal, while the role of the second is to act as catalytic center. One example of this case is the use of MIL-101(Cr,Fe) as solid Lewis acid. MIL-101(Fe) is not stable due to framework flexibility and becomes transformed under reaction conditions into MIL-88B.[111] In contrast MIL-101(Cr) is structurally robust, but Cr^{3+} has lower catalytic activity than Fe^{3+}. A combination of the two metals, Cr and Fe, in the appropriate conditions to ensure stability of the MIL-101 lattice, but with the highest Fe^{3+} content renders a mixed metal MIL-101(Cr,Fe) that is more active as Lewis acid than either MIL-101(Cr) or MIL-101(Fe).[112]

MM-MOFs with mixed-valence metal centers can be formed with one metal center in two different oxidation states. [113-115] The mixed-valence MM-MOFs can find application in oxidation reactions, where the mechanism can involve the swing between two metal oxidation states and aerobic oxidations.[116]

MM-MOFs have also superior photocatalytic performance over homometallic MOFs in various applications such as CO_2 reduction, hydrogen evolution, and pollutant degradation. [78, 117] In MM-MOFs, the introduction of a second metal in the nodes can result in an improvement of the efficiency of the charge transfer from excited states of the ligands to the metal centers or metal oxo clusters, increasing the photocatalytic activity. In fact, the second metal centers can act as an electron mediator introducing a new path for the electron transfer from the ligand to the metal cluster. Such phenomenon has been previously observed in zeolite-anchored bimetallic assemblies or Fe-doped $SrTiO_3$ [118-120] and has been recently claimed to occur in MM NH_2-UiO-66. Thus, series of MM-MOFs based on NH_2-UiO-66(Zr/Ti) with different percentages of exchanged Ti^{4+}

have been synthesized and their behavior has been monitored by transient absorption spectroscopy.[121] Correlation of the transient signal lifetimes with the Ti^{4+} content provides support to the claimed role of Ti^{4+} in MM-MOFs as a mediator to facilitate electron transfer from excited terephthalate ligand to the $(Zr/Ti)_6O_4(OH)_4$ nodes in mixed NH_2-UiO-66(Zr/Ti) MOFs. Furthermore, the observed slow recombination of photogenerated electrons and holes in the mixed NH_2-UiO-66(Zr/Ti) MOFs was beneficial for the construction of a photovoltaic cell fabricated with the mixed NH_2-UiO-66(Zr/Ti), attaining a higher photon-to-current efficiency than the parent NH_2-UiO-66(Zr).

As in the previous case, MM-MOFs can exhibit an enhanced photoresponse compared to their homometallic analogues. Rare-earth containing MOFs provide excellent examples of tunable photoresponsive materials based on MM-MOFs. By introducing into homometallic MOFs, lanthanide metal ions acting as light emitters, novel photoluminescent MM-MOFs can be obtained, exhibiting the intrinsic color emission of dopant. [48] In this way, doping the MOFs with lanthanide metals, such as Tb^{3+} and Eu^{3+} causes intense ligand sensitized luminescence. [122] Moreover, in the mixed Tb–Eu MOFs, upon excitation, energy transfer from Tb^{3+} to Eu^{3+} enhances the Eu^{3+} emissions. [123-125]

Interesting white-light emission has been obtained by Eu−Ag MM-MOF by the adequate combination of a dual-emission, the characteristic red phosphorescence of Eu^{3+} ions and ligand centered emission sensitized by Ag^{+} ion (Figure 17). [126] Also, fine-tuning of the emission to reach the white color characteristic required for lighting applications can be achieved by additional doping of a MOF with intrinsic white light emission with Eu^{3+}ions. [127]

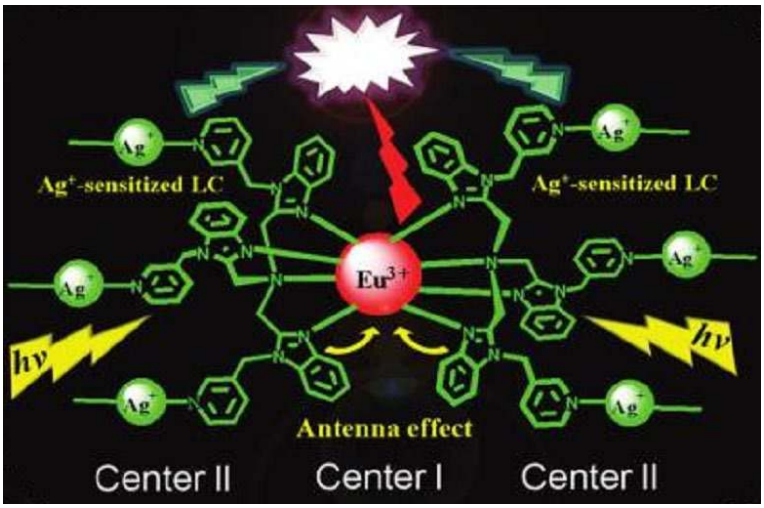

Figure 17. Representation of dual-emitting pathways in Eu-Ag MM-MOF. Ref [[126]]

The Tb-Eu MM-MOFs can be applied as thermometer monitoring the temperature-dependent photoluminescence of the material. Due to the proximity in energy of some excited states, higher energy emissive states can be populated and turned on, increasing their intensity as the temperature increases. On the contrary low temperatures do not allow the population of electronic excited states close but higher in energy and only the emission of the lowest energy excited state can be observed. This phenomenon arises from the temperature-dependent energy-transfer between orbitals of similar energy. Thus, an efficient energy transfer from Tb^{3+} to Eu^{3+} can be achieved at high-temperatures and so the temperature can be correlated to the emission intensity ratio of Tb^{3+} (545 nm) to Eu^{3+} (613 nm). This ratiometric measurement does not require any additional calibration of absolute luminescence intensity. [128, 129]

In the case of gas adsorption, MM-MOFs can also show better performance compared to their homometallic analogues. Ti-exchanged UiO-66 shows 81% enhancement in CO_2 uptake with increased isosteric heat of adsorption.[21] This is due to the inherently stronger adsorption ability of Ti(IV) in comparison to Zr(IV) and also to the increasing charge transfer from the metal to the

ligand which ultimately leads to an increase in CO_2 uptake and enthalpy. Moreover, the somewhat lower framework density of Ti-exchanged UiO-66 results in higher gravimetric CO_2 uptake. In another case, mixed-metal zeolitic imidazolate frameworks (MM-ZIFs) exhibit higher selectivity for CO_2 over CH_4 capture in wet compared to dry conditions. [67] Also, a membrane containing Ti-exchanged UiO-66 composite has 274% and 153% higher CO_2 permeability compared to the values measured for the pristine polymer membrane or the UiO-66 mixed matrix membrane, respectively. It has been proposed that the membrane containing MM-MOFs has a strong interaction between the polymer in the composite and the Ti_xUiO-66 external surface due to the presence of Ti(IV) and this interaction has significant effects on the formation of interfacial free volume generating a significant increase in permeability at the optimal loading (Figure 18). [79]

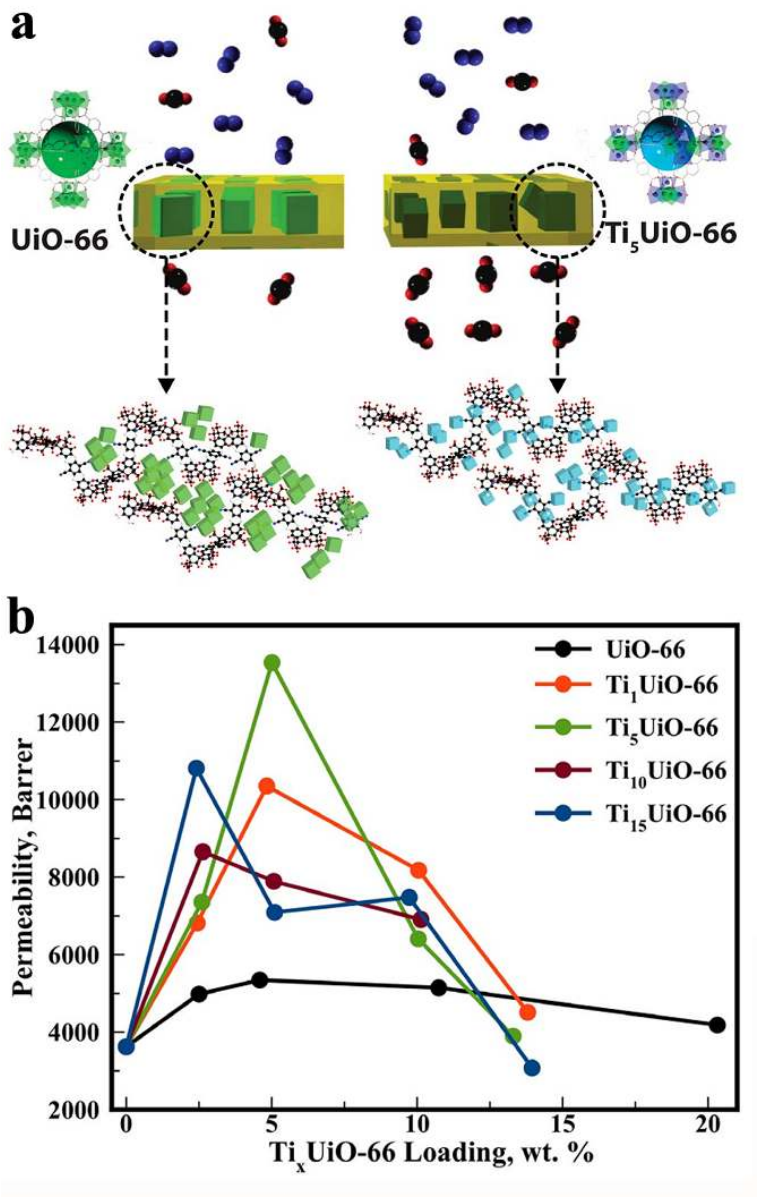

Figure 18. CO_2 Permeability of Ti_xUiO-66 mixed matrix composite membranes. 'x' is the metal exchange incubation period. Ref [[79]]

Existence of different metals in the structure of MM-MOFs can affect to the magnetic behavior of the material compared to homometallic MOF. Moreover, these magnetic properties can be tuned by varying the nature and ratio of the mixed-metal in the MOF. [98] Also, the periodic arrangement of magnetically responsive metals in the pores of MM-MOFs can be responsible for

some unusual properties. For instance, FDM-3 (FDM: Fudan Materials), a mesoporous MM-MOF was prepared by using three geometrically distinct metal-containing SBUs like Cu-based triangular, Zn-based octahedral and Zn-based square pyramidal with an organic linker 4-pyrazolecarboxylate (Figure 19). This combination has resulted in four types of cages in the network with the largest cage of 5.2 nm. Further, this complex architecture with diversified pore environments favors the installation of additional functionalities in the framework as well as accelerates Ag nanoparticle formation.[130]

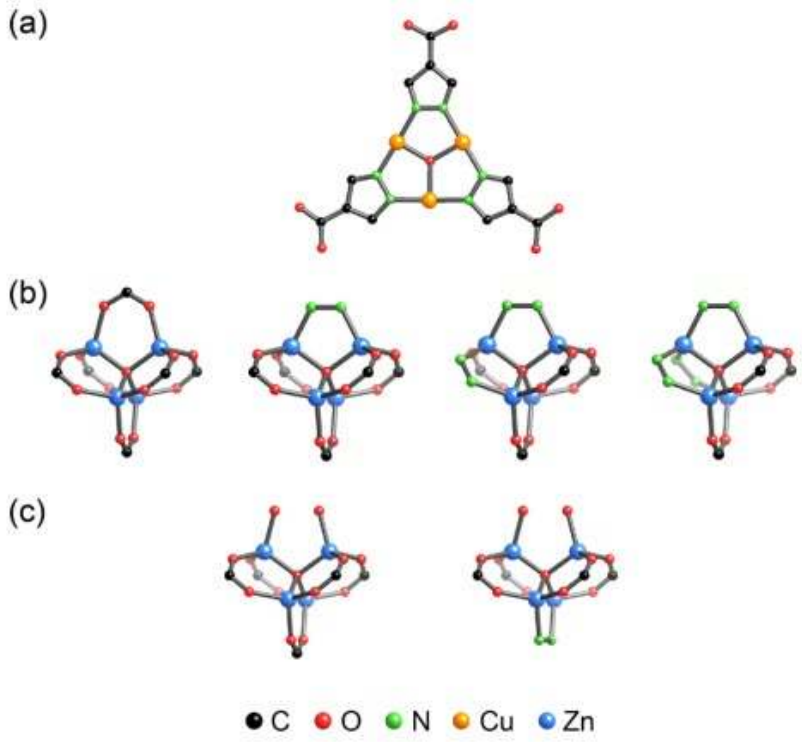

Figure 19. SBUs in FDM-3. (a) One triangular $Cu_3(OH)(PyC)_3$, (b) four octahedral $Zn_4O(COO)_3R_3$ (R = COO or NN), and (c) two square pyramidal $Zn_4O(COO)_4R$. Ref [130]

3.2 Metalloligand MM-MOFs

The metalloligand approach can rationally immobilize into the MM-MOFs different metal sites that can be catalytically or photocatalytically active similarly to soluble molecular complexes. Immobilization by attaching the complexes into the MOF lattice has the general advantage of an increased stability as consequence of the impossibility of complex aggregation that is one common deactivation mechanism occurring in these complexes. [131, 132]

The immobilized metal centers within the micropores of MM-MOFs can exhibit even an enhanced interaction with H_2 molecules, the most challenging case, with an elevated enthalpy at zero coverage. [133] This stronger interaction is derived from the specific environment surrounding the metalloligand and the presence of metal nodes in close proximity. Also, the selectivity and separation properties of MM-MOFs can be tuned and enhanced respect to homometallic MOFs by varying parameters such as immobilization of different metal centers and incorporation of different metal ions as nodes. [133-136]

Easy access to open metal catalytic sites in MM-MOFs constructed with metalloligands [137] makes them highly active solid catalysts in various reactions such as olefin epoxidation, asymmetric alkene epoxidation and acyl-transfer reaction. [138, 139] Again, tunability of such MM-MOFs with various metal catalytic sites makes them more useful for the development of tandem reactions. [137, 139, 140]

Zhou and coworkers have reported the cooperation between nodes and metalloligands in bimetallic PCN-201(Fe)-Cu to promote the Strecker reaction between benzaldehyde, aniline and trimethylsilyl cyanide.[141] PCN-201(Fe)-Cu was prepared stepwise via linker installation and subsequent metalation. Briefly, PCN-224(Fe) was obtained by the metalation of PCN-224 with

$FeCl_2$. Later, the Cu-INA (INA: isonicotinate) units were assembled in PCN-224(Fe) to produce PCN-201(Fe)-Cu MM-MOFs. PCN-201(Fe)-Cu affords 99 % yield of the α-cyanoamine product with a turnover frequency (TOF) of 6000 h^{-1} at room temperature after 10 min. These catalytic data suggest that PCN-201(Fe)-Cu integrates in its structure high valence Fe^{III} and low valence Cu^{I} active centers, which simultaneously activate the electrophiles and nucleophiles at a distance allowing their reaction. In contrast to the performance of PCN-201(Fe)-Cu, PCN-201(Ni)-Cu and PCN-224(Fe) gave 21 and 24 % yield under identical experimental conditions. The low activity of PCN-201(Ni)-Cu MOF that also contains Cu-INA sites, was attributed to the higher Lewis acidity of the Fe-porphyrin center compared to the rather inert Ni-porphyrin. Further, PCN-224(Fe) possesses only Lewis acidic Fe-porphyrin centers, lacking the Cu-INA moieties. Interestingly, the catalytic performance of the physical mixture of PCN-201(Ni)-Cu and PCN-224(Fe) was 68 % that is higher than that of the individual MOFs, but still lower than the activity of PCN-201(Fe)-Cu, showing the advantage of having the two centers in close proximity. Accordingly, even though the physical mixture of PCN-201(Ni)-Cu and PCN-224(Fe) contains both Fe^{III} and Cu^{I} sites to activate electrophiles and nucleophiles, the distance between the two centers makes impossible the reaction between two reagents activated simultaneously. These results unambiguously prove the advantage of MM-MOFs to achieve better performance than their individual components or the corresponding physical mixture.

Recently, an azide-functionalized UiO-66 MOF was used as a platform to immobilize various bidentate ligands on the MOF surface through azide-alkyne cycloaddition reaction. These immobilized bidendate ligands over UiO-66 MOFs form a nickel complex which found to promote Suzuki-Miyaura cross-coupling reactions.[142] The reaction between bromobenzene and phenylboronic acid using UiO-66-(L3)-$Ni(COD)_2$ (L3: 4,4'-bipyridyl, COD: cyclooctadiene)

(Scheme 1) as heterogeneous Ni^{2+}-4,4'-bipyridyl catalyst provided 96 % yield with K_2CO_3 as a base in acetonitrile at 65 °C after 12 h. In contrast, the use of $Ni(COD)_2$ as homogeneous control gave no reaction under identical conditions. Furthermore, UiO-66-N_3 and UiO-66-BPY (BPY: bipyridine) as control catalysts only afforded 5 and 22 % yields of biphenyl under identical conditions. This superior activity of UiO-66-(L3)-$Ni(COD)_2$ was believed to be due to the combination of the highly regular structure of MOF and the well-defined heteroleptic Ni complexes. In contrast, in homogeneous systems with free BPY and PPh_3 ligands in the solution, the selectivity for the formation of the complexes is dictated by the kinetics of ligand exchange under reaction conditions and the thermodynamic stability of each possible homoleptic and heteroleptic complex. Interestingly, the UiO-66-(L3)-$Ni(COD)_2$ catalyst showed identical yield up to seven recycles without any leaching of Ni under reaction conditions.

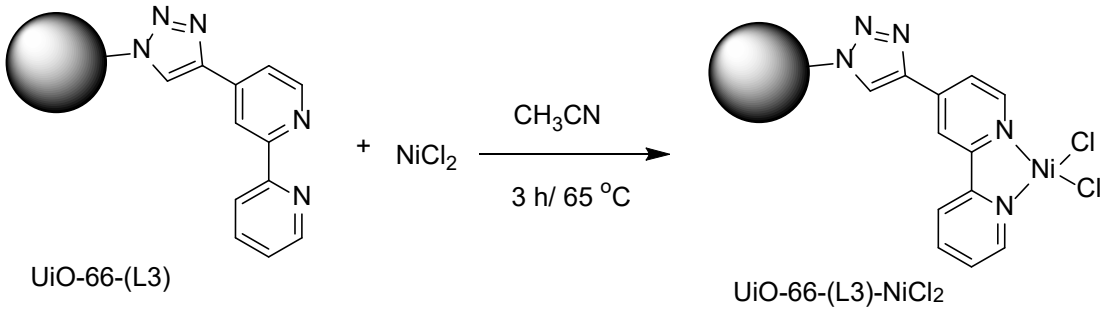

Scheme 1. Schematic representation of the preparation of UiO-66-(L3)-$NiCl_2$. A similar strategy was adopted for the synthesis of UiO-66-(L3)-$Ni(COD)_2$.

A series of stable and porous bipyridyl (BPV) and phenanthryl (PT) MOFs with UiO topology have been prepared and their post-synthetic metalation afforded highly active solid catalysts.[143] For instance, BPV-MOF was obtained with only BPV-functionalized dicarboxylate linker and both mBPV- and mPT-MOFs were constructed with a mixture of BPV or PT-functionalized and unfunctionalized dicarboxylate linkers. These MOFs were post-metalated with

[Ir(COD)(OMe)]$_2$ to obtain BPV-MOF-Ir, mBPV-MOF-Ir, and mPT-MOF-Ir which were employed as catalysts for the C-H borylation of arenes using B_2pin_2 (Scheme 2) and for the tandem hydrosilylation of aryl ketones and aldehydes followed by dehydrogenative ortho-silylation of benzylic silyl ethers. Gratifyingly, mBPV-MOF-Ir provided turnover number of 17000 for C-H borylation of m-xylene with B_2pin_2 and could be recycled more than 15 times without any decay in its activity. Furthermore, the catalytic results have proved that MOF-Ir catalysts exhibited for these reactions 95 times higher reactivity than their homogeneous counterparts, showing the merit of preparing MM-MOFs to favor site isolation within MOFs.

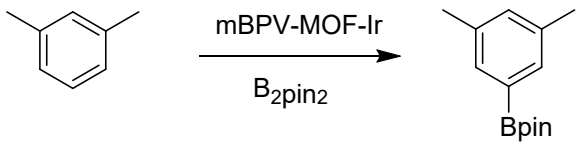

Scheme 2. mBPV-MOF-Ir catalyzed C-H borylation of m-xylene using B_2pin_2.

The metalloligand approach brings the opportunity to synthesize photocatalysts that simultaneously contain photosensitizer units and catalytic sites into a single porous material. For instance, Ru–Pt-UiO-67 MM-MOF, which simultaneously contains a RuBPYDC photosensitizer and a PtBPYDC proton reduction center shows high photocatalytic hydrogen evolution due to the facile electron transfer from the light harvesting Ru-center to the active Pt-reducing center in the MM-MOF (Figure 20). [144] Also various Ir- and Ru-UiO-67 frameworks have been applied for highly effective photocatalytic water oxidation, carbon dioxide photoreduction, and organic photocatalysis evolution. [145]

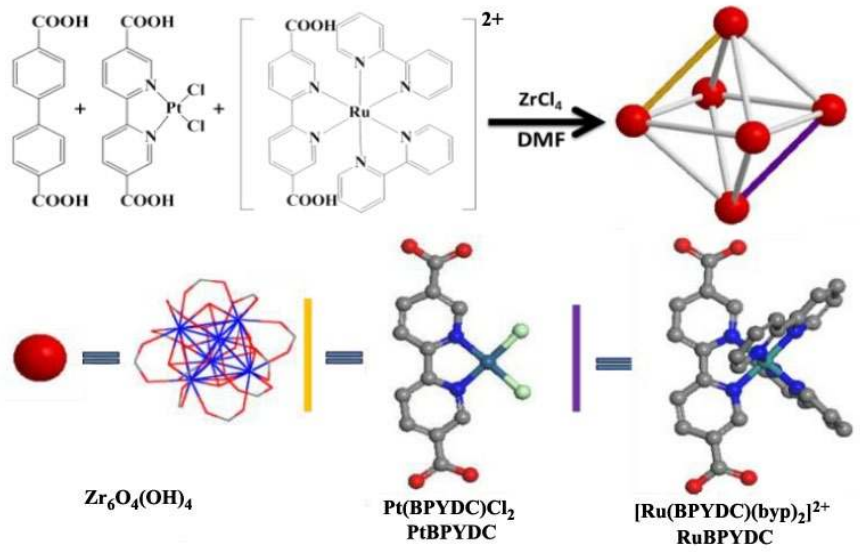

Figure 20. Schematic representation of Ru-Pt-UiO-67 MM-MOF. Ref [[144]]

As mentioned earlier, incorporation of various photoactive metal sites into the MM-MOFs using the metalloligand approach affords photoresponsive materials that can be applied as chemical sensors based on the variation of the emissive properties in the presence of analytes. [146-149]

Also, combination of various chromophores in photoactive MM-MOFs can enhance photoinduced energy transfer processes among the sites. In one of these examples, Os doping in Ru-MM-MOF allows to observe Ru → Os energy-transfer by monitoring the Ru emission at 620 nm, whose lifetime decreased from 171 ns in the pure Ru-MOF to 29 ns in the sample with 2.6 mol % Os doping, observing also an initial growth in Os emission matching the rate of decay of the Ru excited state (Figure 21). [150]

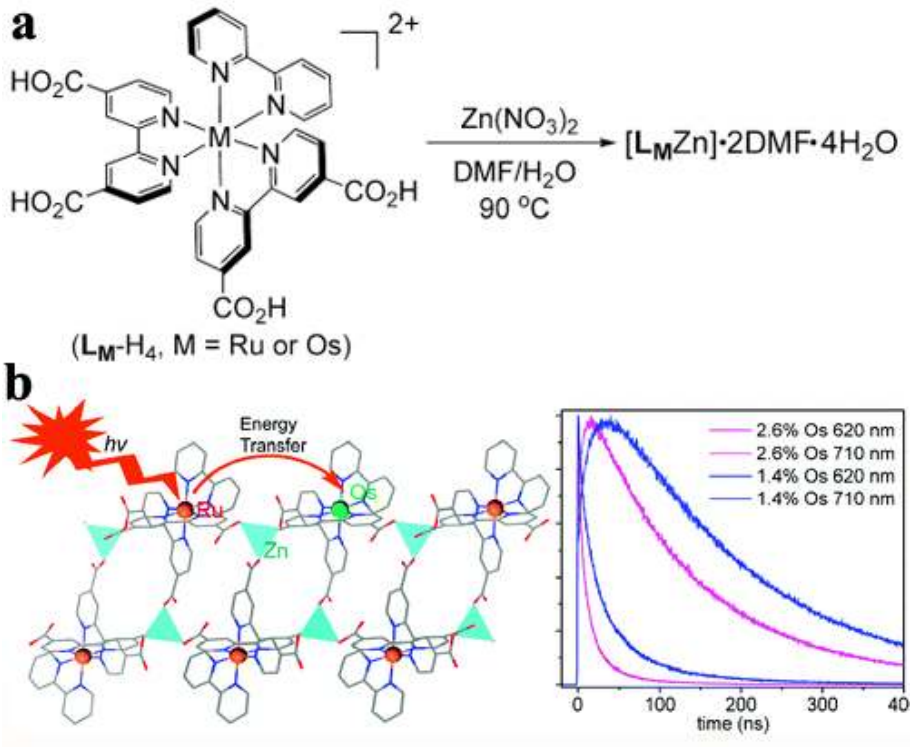

Figure 21. a) Schematic representation for synthesis of L_{Ru}ZnMOF. b) **Left**: X-ray crystal structure of the L_{Ru}Zn MM-MOF showing energy transfer from Ru to Os. **Right**: Emission temperal profile for 1.4 and 2.6 mol % Os-doped L_{Ru}Zn MM-MOFs monitored at 620 and 710 nm with emission at 620 nm dominated by Ru^{II*} and at 710 nm by Os^{II*}. Ref [[150]]

3.3 Metal as a guest in MM-MOFs

In MM-MOFs metal ions, metal nanoparticles, metal complexes, and organometallic compounds can co-exist inside of MOF cavities as guests establishing or not additional interactions between them. In the case of anionic framework of MM-MOFs, there are various metal ions that can be present. Anionic framework of MM-MOFs show enhanced hydrogen adsorption and also cation-dependent kinetic trapping of H_2 due to existence of metal ions hosted within the pores. [20, 84] Also, the anionic framework can serve as a porous support allowing cation exchange to optimize H_2 adsorption enthalpy. Efforts could be focused on construction of such MOFs with an increased

concentration of these metal ion sites. Besides H_2 adsorption, insertion of metal ions inside the MOF framework creates electric dipoles on the surface that render the material suitable for more efficient gas separation. Pd^{2+} and Cu^{2+} complexation with MOF framework exhibit a significantly enhanced selectivity for the adsorption of CO_2 over N_2 compared to the parent MOF (selectivity ratio 2.8 in pristine MOF and 12 in Cu@MOF). [87]

Partial replacement of guest cations in anionic MOFs by lanthanide ions renders these materials photoactive. [85] Also, guest-cation-dependent nonlinear optical activity has been observed upon guest cation exchange with NH_4^+, Na^+, and K^+. [151]

Closely related to metalloligands, metal ions interacting with appropriate functional groups of the organic linker inside MOFs can efficiently catalyze various reactions. For instance, Ti^{4+} ions immobilized on the phenol functional groups of the linkers in the MOF have been reported to catalyze the enantioselective asymmetric addition of $ZnEt_2$ to aromatic aldehydes (Figure 22). [152-154] Pd^{2+} chelating to BPYDC ligand in UiO-67(BPYDC) also catalyzes the carbonylative Sonogashira coupling and Suzuki–Miyaura coupling reaction. [155, 156]

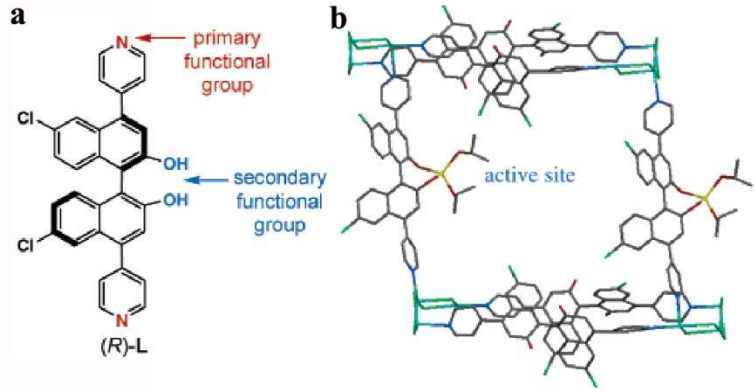

Figure 22. Schematic representation of the a) (R)-6,6′-dichloro-2,2′-dihydroxy-1,1′-binaphthyl-4,4′-bipyridine ligand and b) the active (BINOLate)Ti(O^iPr)$_2$ catalytic sites in the open channels of MOF. Ref [[154]]

Metal nanoparticles incorporated into the cavity of MOFs can also be applied as catalysts or photocatalysts. [157] For example, Pt nanoparticles@Photoactive MOFs have been used for photocatalytic hydrogen evolution [94] and Pd nanoparticles loaded on various MOFs have also been utilized for Suzuki coupling reaction. [95, 158-160] There are in the literature several reviews covering exhaustively the use of MOF encapsulated metal nanoparticles in catalysis and the reader is referred to the existing reports.[93, 157, 161, 162]

In addition, the presence of various metals and rational design of the multifunctional catalysts can allow MM-MOFs to promote cascade or tandem reactions efficiently using only a material containing the necessary active metals in the optimal proportion (Figure 23). For instance, Pd nanoparticles (average size of 1.7 nm) occluded inside MIL-100(Fe) pores, Pd@MIL-100(Fe), exhibited remarkably higher performance in light-induced N-alkylation of amines by alcohols as compared with Pd nanoparticles (6–12 nm) deposited on the external surface of MIL-100(Fe) (Figure 24).[163] In another example, PdAu alloy nanoparticles, which were encapsulated inside MIL-100(Fe) pores, showed higher catalytic activity for light-induced N-alkylation of amines by alcohols in comparison with bare Pd@MIL-100(Fe). The effect of Au can be attributed to the enhancement of the photocatalytic alcohol-to-aldehyde dehydrogenation.[164] Also, in Suzuki coupling reaction bimetallic CuPd nanoclusters encapsulated inside the pores of NH_2-UiO-66(Zr), CuPd@NH_2-UiO-66(Zr), showed higher catalytic efficiency in comparison with Pd@NH_2-UiO-66(Zr).[165] It has been proposed that Cu acts as an electron mediator and facilitates electron transfer from NH_2-UiO-66(Zr) to Pd to create electron-rich metallic Pd.

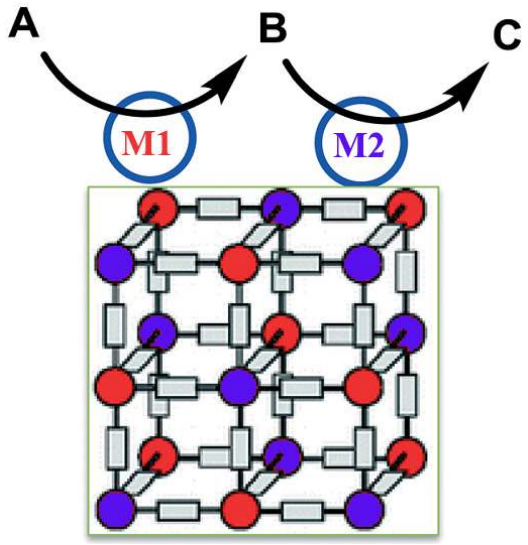

Figure 23. Illustration of the tandem reaction in which each metal (M1 and M2) present in MM-MOFs catalyzes one step.

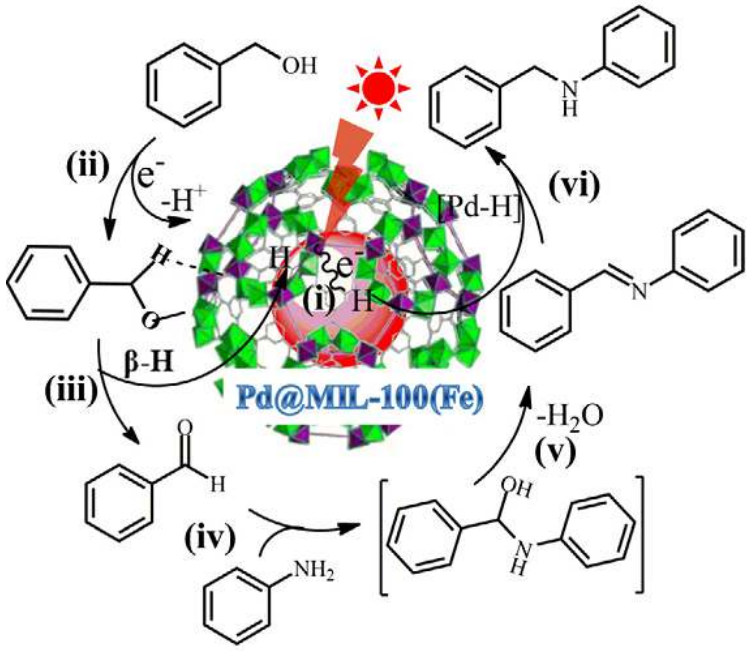

Figure 24. Proposed mechanism for N-alkylation of aniline with benzyl alcohol via hydrogen autotransfer process over Pd@MIL-100(Fe).[164]

Conclusions and Future Prospects

The logical evolution in heterogeneous catalysis is to increase the complexity of materials, tuning their properties to adapt them to the optimal parameters to promote a specific reaction mechanism. This strategy of increased complexity can be more easily implemented in MOFs, because their synthesis can designed with a large predictive capacity. One clear example of this enhanced complexity in material design for enhanced performance is MM-MOFs.

In the present review, it has shown that both methodologies, either one-pot synthesis or post-synthetic modifications have been applied for the preparation of MM-MOFs. Conditions that make these synthesis successful are the similarity in the ionic radii, charge density and softness-hardness nature of the metal ions. However, a clearer picture of the conditions and limitations of both strategies as well as when the MM-MOF formation is controlled by thermodynamics or kinetics is still missing in the area. The field is also needed of more examples addressing a detailed characterization of the location of the second metal in the structure, particularly compelling evidence of the occurrence of nodal exchange vs. location at satellite positions.

Because MM-MOFs as MTV-MOFs represent a higher degree of complexity than homometallic MOFs they frequently show superior advantages over simple MOFs with respect to their properties and applications. Examples have been presented showing how by introducing another metal ion to a homometallic MOF, new properties and activity due to the presence of the second metal ion can be observed, along with the occurrence of synergic effects on the resulting MM-MOF. These MM-MOFs show enhancement in porosity and gas uptake, improvement in permeability, promotion of catalytic and photocatalytic properties, and tunable magnetic behavior

while bringing about adjustable photoactive properties. It has been shown that MM-MOFs are particularly promising as catalysts for tandem reactions, since each type of metal can be active site for one of the elementary steps in the tandem. Also, MM-MOFs can serve as precursors of binary, ternary and quaternary metal oxide nanoparticles with excellent control over stoichiometry and particle size.

Considering the large diversity of MOF structures and the various possibilities that these materials offer to introduce additional metals by exchange or incorporation, it can be predicted that this area will grow in the near future to bring the performance of the MM-MOF in areas like adsorption, separation and catalysis much beyond that achieved with homometallic MOFs.

Acknowledgements:

Support of this investigation by Tarbiat Modares University is gratefully acknowledged. AD thanks the University Grants Commission, New Delhi, for the award of an Assistant Professorship under its Faculty Recharge Programme. AD also thanks the Department of Science and Technology, India, for the financial support through Extra Mural Research Funding (EMR/2016/006500). Financial support by the Spanish Ministry of Economy and Competitiveness (Severo Ochoa and CTQ2015-69153-CO2-1) and Generalitat Valenciana (Prometeo 2017-083) is gratefully acknowledged.

References

[1] M. Eddaoudi, J. Kim, N. Rosi, D. Vodak, J. Wachter, M. O'keeffe, O. M. Yaghi, *Science* **2002**, *295*, 469-72.

[2] J. S. Seo, D. Whang, H. Lee, S. Im Jun, J. Oh, J. Y. Jeon, K. Kim, *Nature* **2000**, *404*, 982-6.

[3] G. Férey, C. Mellot-Draznieks, C. Serre, F. Millange, J. Dutour, S. Surblé, I. Margiolaki, *Science* **2005**, *309*, 2040-2.
[4] M. Y. Masoomi, A. Morsali, *RSC Advances* **2013**, *3*, 19191-218.
[5] M. Y. Masoomi, M. Bagheri, A. Morsali, *Ultrasonics Sonochemistry* **2017**, *37*, 244-50.
[6] M. Y. Masoomi, M. Bagheri, A. Morsali, *RSC Advances* **2016**, *6*, 13272-7.
[7] E. Tahmasebi, M. Y. Masoomi, Y. Yamini, A. Morsali, *RSC Advances* **2016**, *6*, 40211-8.
[8] M. Safari, Y. Yamini, M. Y. Masoomi, A. Morsali, A. Mani-Varnosfaderani, *Microchimica Acta* **2017**, *184*, 1555-64.
[9] M. S. Rahmanifar, H. Hesari, A. Noori, M. Y. Masoomi, A. Morsali, M. F. Mousavi, *Electrochimica Acta* **2018**, *275*, 76-86.
[10] M. Bagheri, M. Y. Masoomi, A. Morsali, *Journal of Hazardous materials* **2017**, *331*, 142-9.
[11] M. Bagheri, M. Y. Masoomi, A. Morsali, *ACS Catalysis* **2017**, 6949-56.
[12] S. A. A. Razavi, M. Y. Masoomi, T. Islamoglu, A. Morsali, Y. Xu, J. T. Hupp, O. K. Farha, J. Wang, P. C. Junk, *Inorganic Chemistry* **2017**, *56*, 2581-8.
[13] S. A. A. Razavi, M. Y. Masoomi, A. Morsali, *Chemistry – A European Journal* **2017**, *23*, 12559-64.
[14] T. R. Cook, Y.-R. Zheng, P. J. Stang, *Chemical Reviews* **2013**, *113*, 734-77.
[15] H. Furukawa, U. Müller, O. M. Yaghi, *Angewandte Chemie International Edition* **2015**, *54*, 3417-30.
[16] M. C. Das, S. Xiang, Z. Zhang, B. Chen, *Angewandte Chemie International Edition* **2011**, *50*, 10510-20.
[17] B. Zhao, X.-Y. Chen, P. Cheng, D.-Z. Liao, S.-P. Yan, Z.-H. Jiang, *Journal of the American Chemical Society* **2004**, *126*, 15394-5.
[18] H. Guo, Y. Zhu, S. Qiu, J. A. Lercher, H. Zhang, *Advanced Materials* **2010**, *22*, 4190-2.
[19] G.-T. Vuong, M.-H. Pham, T.-O. Do, *Dalton Transactions* **2013**, *42*, 550-7.
[20] M. Dincă, J. R. Long, *Journal of the American Chemical Society* **2007**, *129*, 11172-6.
[21] C. Hon Lau, R. Babarao, M. R. Hill, *Chemical Communications* **2013**, *49*, 3634-6.
[22] B. Chen, S. Xiang, G. Qian, *Accounts of Chemical Research* **2010**, *43*, 1115-24.
[23] H. Furukawa, K. E. Cordova, M. O'Keeffe, O. M. Yaghi, *Science* **2013**, *341*, 1230444.
[24] K. M. Choi, H. M. Jeong, J. H. Park, Y.-B. Zhang, J. K. Kang, O. M. Yaghi, *ACS Nano* **2014**, *8*, 7451-7.
[25] Y. Jiao, C. R. Morelock, N. C. Burtch, W. P. Mounfield, J. T. Hungerford, K. S. Walton, *Industrial & Engineering Chemistry Research* **2015**, *54*, 12408-14.
[26] N. Stock, S. Biswas, *Chemical Reviews* **2012**, *112*, 933-69.
[27] A. Dhakshinamoorthy, A. M. Asiri, H. Garcia, *Catalysis Science & Technology* **2016**, *6*, 5238-61.
[28] B. Li, Y. Xie, J. Huang, Y. Qian, *Advanced Materials* **1999**, *11*, 1456-9.
[29] Y. Yue, P. F. Fulvio, S. Dai, *Accounts of Chemical Research* **2015**, *48*, 3044-52.
[30] M. Y. Masoomi, K. C. Stylianou, A. Morsali, P. Retailleau, D. Maspoch, *Crystal Growth & Design* **2014**, *14*, 2092-6.
[31] V. Safarifard, A. Morsali, *Coordination Chemistry Reviews* **2015**, *292*, 1-14.
[32] S. A. A. Razavi, M. Y. Masoomi, A. Morsali, *Ultrasonics Sonochemistry* **2017**, *37*, 502-8.
[33] S. R. Caskey, A. J. Matzger, *Inorganic Chemistry* **2008**, *47*, 7942-4.
[34] X.-J. Kong, Y.-P. Ren, L.-S. Long, R.-B. Huang, L.-S. Zheng, M. Kurmoo, *CrystEngComm* **2008**, *10*, 1309-14.
[35] Y. Wang, B. Bredenkotter, B. Rieger, D. Volkmer, *Dalton Transactions* **2007**, 689-96.
[36] J. He, J. Yu, Y. Zhang, Q. Pan, R. Xu, *Inorganic Chemistry* **2005**, *44*, 9279-82.
[37] Y. Zhang, B. Chen, F. R. Fronczek, A. W. Maverick, *Inorganic Chemistry* **2008**, *47*, 4433-5.
[38] A. Schoedel, A. J. Cairns, Y. Belmabkhout, L. Wojtas, M. Mohamed, Z. Zhang, D. M. Proserpio, M. Eddaoudi, M. J. Zaworotko, *Angewandte Chemie International Edition* **2013**, *52*, 2902-5.

[39] S. Horike, R. Matsuda, D. Tanaka, S. Matsubara, M. Mizuno, K. Endo, S. Kitagawa, *Angewandte Chemie International Edition* **2006**, *45*, 7226-30.
[40] S. Nayak, K. Harms, S. Dehnen, *Inorganic Chemistry* **2011**, *50*, 2714-6.
[41] Z. Su, Z.-S. Bai, J. Fan, J. Xu, W.-Y. Sun, *Crystal Growth & Design* **2009**, *9*, 5190-6.
[42] L. J. Wang, H. Deng, H. Furukawa, F. Gándara, K. E. Cordova, D. Peri, O. M. Yaghi, *Inorganic Chemistry* **2014**, *53*, 5881-3.
[43] P.-F. Shi, H.-C. Hu, Z.-Y. Zhang, G. Xiong, B. Zhao, *Chemical Communications* **2015**, *51*, 3985-8.
[44] F.-N. Shi, A. R. Silva, T.-H. Yang, J. Rocha, *CrystEngComm* **2013**, *15*, 3776-9.
[45] J. A. Botas, G. Calleja, M. Sánchez-Sánchez, M. G. Orcajo, *Langmuir* **2010**, *26*, 5300-3.
[46] W.-C. Song, J.-R. Li, P.-C. Song, Y. Tao, Q. Yu, X.-L. Tong, X.-H. Bu, *Inorganic Chemistry* **2009**, *48*, 3792-9.
[47] C. Serre, F. Millange, C. Thouvenot, N. Gardant, F. Pelle, G. Ferey, *Journal of Materials Chemistry* **2004**, *14*, 1540-3.
[48] P. Falcaro, S. Furukawa, *Angewandte Chemie International Edition* **2012**, *51*, 8431-3.
[49] C. Livage, P. M. Forster, N. Guillou, M. M. Tafoya, A. K. Cheetham, G. Férey, *Angewandte Chemie International Edition* **2007**, *46*, 5877-9.
[50] L. Xie, S. Liu, C. Gao, R. Cao, J. Cao, C. Sun, Z. Su, *Inorganic Chemistry* **2007**, *46*, 7782-8.
[51] J. H. Yoon, S. B. Choi, Y. J. Oh, M. J. Seo, Y. H. Jhon, T.-B. Lee, D. Kim, S. H. Choi, J. Kim, *Catalysis Today* **2007**, *120*, 324-9.
[52] Y.-Z. Zheng, W. Xue, W.-X. Zhang, M.-L. Tong, X.-M. Chen, F. Grandjean, G. J. Long, S.-W. Ng, P. Panissod, M. Drillon, *Inorganic Chemistry* **2009**, *48*, 2028-42.
[53] X.-M. Zhang, Y.-Z. Zheng, C.-R. Li, W.-X. Zhang, X.-M. Chen, *Crystal Growth & Design* **2007**, *7*, 980-3.
[54] J. Jia, X. Lin, C. Wilson, A. J. Blake, N. R. Champness, P. Hubberstey, G. Walker, E. J. Cussen, M. Schroder, *Chemical Communications* **2007**, 840-2.
[55] J. r. Lincke, D. Lässig, M. Kobalz, J. Bergmann, M. Handke, J. Möllmer, M. Lange, C. Roth, A. Möller, R. Staudt, *Inorganic Chemistry* **2012**, *51*, 7579-86.
[56] F.-N. Shi, L. s. Cunha-Silva, T. Trindade, F. A. A. Paz, J. Rocha, *Crystal Growth and Design* **2009**, *9*, 2098-109.
[57] M. Lammert, C. Glißmann, N. Stock, *Dalton Transactions* **2017**, *46*, 2425-9.
[58] V. Sridharan, J. C. Menéndez, *Chemical Reviews* **2010**, *110*, 3805-49.
[59] Y. Ren, X. Cheng, S. Yang, C. Qi, H. Jiang, Q. Mao, *Dalton Transactions* **2013**, *42*, 9930-7.
[60] S. R. Halper, L. Do, J. R. Stork, S. M. Cohen, *Journal of the American Chemical Society* **2006**, *128*, 15255-68.
[61] M. C. Das, Q. Guo, Y. He, J. Kim, C.-G. Zhao, K. Hong, S. Xiang, Z. Zhang, K. M. Thomas, R. Krishna, B. Chen, *Journal of the American Chemical Society* **2012**, *134*, 8703-10.
[62] A. Schoedel, L. Wojtas, S. P. Kelley, R. D. Rogers, M. Eddaoudi, M. J. Zaworotko, *Angewandte Chemie International Edition* **2011**, *50*, 11421-4.
[63] D. L. Murphy, M. R. Malachowski, C. F. Campana, S. M. Cohen, *Chemical Communications* **2005**, 5506-8.
[64] B. Chen, F. R. Fronczek, A. W. Maverick, *Inorganic Chemistry* **2004**, *43*, 8209-11.
[65] S. R. Halper, S. M. Cohen, *Inorganic Chemistry* **2005**, *44*, 486-8.
[66] J. R. Stork, V. S. Thoi, S. M. Cohen, *Inorganic Chemistry* **2007**, *46*, 11213-23.
[67] N. T. Nguyen, T. N. Lo, J. Kim, H. T. Nguyen, T. B. Le, K. E. Cordova, H. Furukawa, *Inorganic Chemistry* **2016**, *55*, 6201-7.
[68] W. Yuan, J. O'Connor, S. L. James, *CrystEngComm* **2010**, *12*, 3515-7.
[69] M.-H. Xie, X.-L. Yang, C. Zou, C.-D. Wu, *Inorganic Chemistry* **2011**, *50*, 5318-20.

[70] Q. Lin, X. Bu, A. Kong, C. Mao, X. Zhao, F. Bu, P. Feng, *Journal of the American Chemical Society* **2015**, *137*, 2235-8.
[71] Q. Liu, H. Cong, H. Deng, *Journal of the American Chemical Society* **2016**, *138*, 13822-5.
[72] M. Lalonde, W. Bury, O. Karagiaridi, Z. Brown, J. T. Hupp, O. K. Farha, *Journal of Materials Chemistry A* **2013**, *1*, 5453-68.
[73] S. Furukawa, K. Hirai, K. Nakagawa, Y. Takashima, R. Matsuda, T. Tsuruoka, M. Kondo, R. Haruki, D. Tanaka, H. Sakamoto, S. Shimomura, O. Sakata, S. Kitagawa, *Angewandte Chemie International Edition* **2009**, *48*, 1766-70.
[74] X. Song, T. K. Kim, H. Kim, D. Kim, S. Jeong, H. R. Moon, M. S. Lah, *Chemistry of Materials* **2012**, *24*, 3065-73.
[75] B. Tu, Q. Pang, D. Wu, Y. Song, L. Weng, Q. Li, *Journal of the American Chemical Society* **2014**, *136*, 14465-71.
[76] A. M. Shultz, A. A. Sarjeant, O. K. Farha, J. T. Hupp, S. T. Nguyen, *Journal of the American Chemical Society* **2011**, *133*, 13252-5.
[77] P. Deria, J. E. Mondloch, O. Karagiaridi, W. Bury, J. T. Hupp, O. K. Farha, *Chemical Society Reviews* **2014**, *43*, 5896-912.
[78] D. Sun, W. Liu, M. Qiu, Y. Zhang, Z. Li, *Chemical Communications* **2015**, *51*, 2056-9.
[79] S. J. D. Smith, B. P. Ladewig, A. J. Hill, C. H. Lau, M. R. Hill, *Scientific Reports* **2015**, *5*, 7823.
[80] S. Das, H. Kim, K. Kim, *Journal of the American Chemical Society* **2009**, *131*, 3814-5.
[81] F. Vermoortele, B. Bueken, G. Le Bars, B. Van de Voorde, M. Vandichel, K. Houthoofd, A. Vimont, M. Daturi, M. Waroquier, V. Van Speybroeck, C. Kirschhock, D. E. De Vos, *Journal of the American Chemical Society* **2013**, *135*, 11465-8.
[82] M. Kim, J. F. Cahill, H. Fei, K. A. Prather, S. M. Cohen, *Journal of the American Chemical Society* **2012**, *134*, 18082-8.
[83] J. G. Santaclara, A. I. Olivos-Suarez, A. Gonzalez-Nelson, D. Osadchii, M. A. Nasalevich, M. A. van der Veen, F. Kapteijn, A. M. Sheveleva, S. L. Veber, M. V. Fedin, A. T. Murray, C. H. Hendon, A. Walsh, J. Gascon, *Chemistry of Materials* **2017**, *29*, 8963-7.
[84] S. Yang, X. Lin, A. J. Blake, G. S. Walker, P. Hubberstey, N. R. Champness, M. Schröder, *Nat Chem* **2009**, *1*, 487-93.
[85] J.-S. Qin, S.-R. Zhang, D.-Y. Du, P. Shen, S.-J. Bao, Y.-Q. Lan, Z.-M. Su, *Chemistry – A European Journal* **2014**, *20*, 5625-30.
[86] X.-P. Zhou, Z. Xu, M. Zeller, A. D. Hunter, *Chemical Communications* **2009**, 5439-41.
[87] E. D. Bloch, D. Britt, C. Lee, C. J. Doonan, F. J. Uribe-Romo, H. Furukawa, J. R. Long, O. M. Yaghi, *Journal of the American Chemical Society* **2010**, *132*, 14382-4.
[88] J. S. Seo, D. Whang, H. Lee, S. Im Jun, *Nature* **2000**, *404*, 982.
[89] M. I. Gonzalez, E. D. Bloch, J. A. Mason, S. J. Teat, J. R. Long, *Inorganic Chemistry* **2015**, *54*, 2995-3005.
[90] S. Hermes, M.-K. Schröter, R. Schmid, L. Khodeir, M. Muhler, A. Tissler, R. W. Fischer, R. A. Fischer, *Angewandte Chemie International Edition* **2005**, *44*, 6237-41.
[91] S. Hermes, F. Schroder, S. Amirjalayer, R. Schmid, R. A. Fischer, *Journal of Materials Chemistry* **2006**, *16*, 2464-72.
[92] M. Muller, O. I. Lebedev, R. A. Fischer, *Journal of Materials Chemistry* **2008**, *18*, 5274-81.
[93] M. Meilikhov, K. Yusenko, D. Esken, S. Turner, G. Van Tendeloo, R. A. Fischer, *European Journal of Inorganic Chemistry* **2010**, *2010*, 3701-14.
[94] C. Wang, K. E. deKrafft, W. Lin, *Journal of the American Chemical Society* **2012**, *134*, 7211-4.
[95] D. Sun, Z. Li, *The Journal of Physical Chemistry C* **2016**, *120*, 19744-50.
[96] M. Meilikhov, K. Yusenko, A. Torrisi, B. Jee, C. Mellot-Draznieks, A. Pöppl, R. A. Fischer, *Angewandte Chemie International Edition* **2010**, *49*, 6212-5.

[97] G. Férey, F. Millange, M. Morcrette, C. Serre, M. L. Doublet, J. M. Grenèche, J. M. Tarascon, *Angewandte Chemie International Edition* **2007**, *46*, 3259-63.
[98] M.-H. Zeng, B. Wang, X.-Y. Wang, W.-X. Zhang, X.-M. Chen, S. Gao, *Inorganic Chemistry* **2006**, *45*, 7069-76.
[99] M. Y. Masoomi, A. Morsali, *Coordination Chemistry Reviews* **2012**, *256*, 2921-43.
[100] S. Chen, M. Xue, Y. Li, Y. Pan, L. Zhu, D. Zhang, Q. Fang, S. Qiu, *Inorganic Chemistry Frontiers* **2015**, *2*, 177-83.
[101] A. Dhakshinamoorthy, A. M. Asiri, H. Garcia, *ACS Catalysis* **2019**, *9*, 1081-102.
[102] A. Dhakshinamoorthy, Z. Li, H. Garcia, *Chemical Society Reviews* **2018**, *47*, 8134-72.
[103] L. Zhu, X.-Q. Liu, H.-L. Jiang, L.-B. Sun, *Chemical Reviews* **2017**, *117*, 8129-76.
[104] M. Giménez-Marqués, A. Santiago-Portillo, S. Navalón, M. Álvaro, F. Nouar, H. Garcia, C. Serre, *unpublished results*.
[105] D. Sun, F. Sun, X. Deng, Z. Li, *Inorganic Chemistry* **2015**, *54*, 8639-43.
[106] C. P. Krap, R. Newby, A. Dhakshinamoorthy, H. García, I. Cebula, T. L. Easun, M. Savage, J. E. Eyley, S. Gao, A. J. Blake, W. Lewis, P. H. Beton, M. R. Warren, D. R. Allan, M. D. Frogley, C. C. Tang, G. Cinque, S. Yang, M. Schröder, *Inorganic Chemistry* **2016**, *55*, 1076-88.
[107] M. R. Ghaleno, M. Ghaffari-Moghaddam, M. Khajeh, A. R. Oveisi, M. Bohlooli, *Journal of colloid and interface science* **2019**, *535*, 214-26.
[108] L. M. Aguirre-Díaz, F. Gándara, M. Iglesias, N. Snejko, E. Gutiérrez-Puebla, M. Á. Monge, *Journal of the American Chemical Society* **2015**, *137*, 6132-5.
[109] L. Mitchell, P. Williamson, B. Ehrlichová, A. E. Anderson, V. R. Seymour, S. E. Ashbrook, N. Acerbi, L. M. Daniels, R. I. Walton, M. L. Clarke, *Chemistry–A European Journal* **2014**, *20*, 17185-97.
[110] M. Yadollahi, H. Hamadi, V. Nobakht, *Applied Organometallic Chemistry* **2019**, *33*, e4819.
[111] A. Schneemann, V. Bon, I. Schwedler, I. Senkovska, S. Kaskel, R. A. Fischer, *Chemical Society Reviews* **2014**, *43*, 6062-96.
[112] M. Alvaro, S. Navalon, H. Garcia, *unpublished results.*
[113] J. He, J.-X. Zhang, C.-K. Tsang, Z. Xu, Y.-G. Yin, D. Li, S.-W. Ng, *Inorganic Chemistry* **2008**, *47*, 7948-50.
[114] S.-S. Chen, Q. Liu, Y. Zhao, R. Qiao, L.-Q. Sheng, Z.-D. Liu, S. Yang, C.-F. Song, *Crystal Growth & Design* **2014**, *14*, 3727-41.
[115] M. I. Breeze, G. Clet, B. C. Campo, A. Vimont, M. Daturi, J.-M. Grenèche, A. J. Dent, F. Millange, R. I. Walton, *Inorganic Chemistry* **2013**, *52*, 8171-82.
[116] P. Kar, R. Haldar, C. J. Gómez-García, A. Ghosh, *Inorganic Chemistry* **2012**, *51*, 4265-73.
[117] M. Y. Masoomi, M. Bagheri, A. Morsali, P. C. Junk, *Inorganic Chemistry Frontiers* **2016**, *3*, 944-51.
[118] T.-H. Xie, X. Sun, J. Lin, *The Journal of Physical Chemistry C* **2008**, *112*, 9753-9.
[119] W. Lin, H. Frei, *Journal of the American Chemical Society* **2005**, *127*, 1610-1.
[120] R. Nakamura, A. Okamoto, H. Osawa, H. Irie, K. Hashimoto, *Journal of the American Chemical Society* **2007**, *129*, 9596-7.
[121] A. Santiago Portillo, H. G. Baldoví, M. T. Garcia Fernandez, S. Navalón, P. Atienzar, B. Ferrer, M. Alvaro, H. Garcia, Z. Li, *The Journal of Physical Chemistry C* **2017**, *121*, 7015-24.
[122] A. Thirumurugan, A. K. Cheetham, *European Journal of Inorganic Chemistry* **2010**, *2010*, 3823-8.
[123] D. Sarma, M. Prabu, S. Biju, M. L. P. Reddy, S. Natarajan, *European Journal of Inorganic Chemistry* **2010**, *2010*, 3813-22.
[124] D. T. de Lill, A. de Bettencourt-Dias, C. L. Cahill, *Inorganic Chemistry* **2007**, *46*, 3960-5.
[125] P. C. R. Soares-Santos, L. Cunha-Silva, F. A. A. Paz, R. A. S. Ferreira, J. Rocha, T. Trindade, L. D. Carlos, H. I. S. Nogueira, *Crystal Growth & Design* **2008**, *8*, 2505-16.
[126] Y. Liu, M. Pan, Q.-Y. Yang, L. Fu, K. Li, S.-C. Wei, C.-Y. Su, *Chemistry of Materials* **2012**, *24*, 1954-60.

[127] D. F. Sava, L. E. S. Rohwer, M. A. Rodriguez, T. M. Nenoff, *Journal of the American Chemical Society* **2012**, *134*, 3983-6.
[128] Y. Cui, H. Xu, Y. Yue, Z. Guo, J. Yu, Z. Chen, J. Gao, Y. Yang, G. Qian, B. Chen, *Journal of the American Chemical Society* **2012**, *134*, 3979-82.
[129] X. Rao, T. Song, J. Gao, Y. Cui, Y. Yang, C. Wu, B. Chen, G. Qian, *Journal of the American Chemical Society* **2013**, *135*, 15559-64.
[130] B. Tu, Q. Pang, E. Ning, W. Yan, Y. Qi, D. Wu, Q. Li, *Journal of the American Chemical Society* **2015**, *137*, 13456-9.
[131] R. Kitaura, G. Onoyama, H. Sakamoto, R. Matsuda, S.-i. Noro, S. Kitagawa, *Angewandte Chemie* **2004**, *116*, 2738-41.
[132] H. Sakamoto, R. Matsuda, S. Bureekaew, D. Tanaka, S. Kitagawa, *Chemistry-A European Journal* **2009**, *15*, 4985-9.
[133] B. Chen, X. Zhao, A. Putkham, K. Hong, E. B. Lobkovsky, E. J. Hurtado, A. J. Fletcher, K. M. Thomas, *Journal of the American Chemical Society* **2008**, *130*, 6411-23.
[134] J. Ferrando-Soria, P. Serra-Crespo, M. de Lange, J. Gascon, F. Kapteijn, M. Julve, J. Cano, F. Lloret, J. Pasán, C. Ruiz-Pérez, Y. Journaux, E. Pardo, *Journal of the American Chemical Society* **2012**, *134*, 15301-4.
[135] S.-C. Xiang, Z. Zhang, C.-G. Zhao, K. Hong, X. Zhao, D.-R. Ding, M.-H. Xie, C.-D. Wu, M. C. Das, R. Gill, *Nature Communications* **2011**, *2*, 204.
[136] Z. Zhang, S. Xiang, K. Hong, M. C. Das, H. D. Arman, M. Garcia, J. U. Mondal, K. M. Thomas, B. Chen, *Inorganic Chemistry* **2012**, *51*, 4947-53.
[137] A. M. Shultz, O. K. Farha, J. T. Hupp, S. T. Nguyen, *Journal of the American Chemical Society* **2009**, *131*, 4204-5.
[138] S.-H. Cho, B. Ma, S. T. Nguyen, J. T. Hupp, T. E. Albrecht-Schmitt, *Chemical Communications* **2006**, 2563-5.
[139] F. Song, C. Wang, J. M. Falkowski, L. Ma, W. Lin, *Journal of the American Chemical Society* **2010**, *132*, 15390-8.
[140] L. Chen, S. Rangan, J. Li, H. Jiang, Y. Li, *Green Chemistry* **2014**, *16*, 3978-85.
[141] Y. Peng, H. Huang, Y. Zhang, C. Kang, S. Chen, L. Song, D. Liu, C. Zhong, *Nature communications* **2018**, *9*, 187.
[142] P. Elumalai, H. Mamlouk, W. Yiming, L. Feng, S. Yuan, H.-C. Zhou, S. T. Madrahimov, *ACS applied materials & interfaces* **2018**, *10*, 41431-8.
[143] K. Manna, T. Zhang, F. X. Greene, W. Lin, *Journal of the American Chemical Society* **2015**, *137*, 2665-73.
[144] C.-C. Hou, T.-T. Li, S. Cao, Y. Chen, W.-F. Fu, *Journal of Materials Chemistry A* **2015**, *3*, 10386-94.
[145] C. Wang, Z. Xie, K. E. deKrafft, W. Lin, *Journal of the American Chemical Society* **2011**, *133*, 13445-54.
[146] B. D. Chandler, A. P. Cote, D. T. Cramb, J. M. Hill, G. K. H. Shimizu, *Chemical Communications* **2002**, 1900-1.
[147] B. D. Chandler, D. T. Cramb, G. K. H. Shimizu, *Journal of the American Chemical Society* **2006**, *128*, 10403-12.
[148] B. D. Chandler, J. O. Yu, D. T. Cramb, G. K. H. Shimizu, *Chemistry of Materials* **2007**, *19*, 4467-73.
[149] Z. Xie, L. Ma, K. E. deKrafft, A. Jin, W. Lin, *Journal of the American Chemical Society* **2010**, *132*, 922-3.
[150] C. A. Kent, B. P. Mehl, L. Ma, J. M. Papanikolas, T. J. Meyer, W. Lin, *Journal of the American Chemical Society* **2010**, *132*, 12767-9.
[151] Y. Liu, G. Li, X. Li, Y. Cui, *Angewandte Chemie* **2007**, *119*, 6417-20.
[152] C.-D. Wu, W. Lin, *Angewandte Chemie* **2007**, *119*, 1093-6.

[153] L. Ma, C.-D. Wu, M. M. Wanderley, W. Lin, *Angewandte Chemie* **2010**, *122*, 8420-4.
[154] C.-D. Wu, A. Hu, L. Zhang, W. Lin, *Journal of the American Chemical Society* **2005**, *127*, 8940-1.
[155] C. Bai, S. Jian, X. Yao, Y. Li, *Catalysis Science & Technology* **2014**, *4*, 3261-7.
[156] H. Fei, S. M. Cohen, *Chemical Communications* **2014**, *50*, 4810-2.
[157] A. Dhakshinamoorthy, H. Garcia, *Chemical Society Reviews* **2012**, *41*, 5262-84.
[158] B. Yuan, Y. Pan, Y. Li, B. Yin, H. Jiang, *Angewandte Chemie International Edition* **2010**, *49*, 4054-8.
[159] Y. Huang, Z. Zheng, T. Liu, J. Lü, Z. Lin, H. Li, R. Cao, *Catalysis Communications* **2011**, *14*, 27-31.
[160] M. Zhang, J. Guan, B. Zhang, D. Su, C. Williams, C. Liang, *Catalysis Letters* **2012**, *142*, 313-8.
[161] Q. Yang, Q. Xu, H.-L. Jiang, *Chemical Society Reviews* **2017**, *46*, 4774-808.
[162] A. Dhakshinamoorthy, A. M. Asiri, H. Garcia, *ACS Catalysis* **2017**, *7*, 2896-919.
[163] D. Wang, Z. Li, *Journal of catalysis* **2016**, *342*, 151-7.
[164] D. Wang, Y. Pan, L. Xu, Z. Li, *Journal of Catalysis* **2018**, *361*, 248-54.
[165] D. Sun, M. Xu, Y. Jiang, J. Long, Z. Li, *Small Methods* **2018**, *2*, 1800164.